Microglia-secreted TNF-α affects differentiation efficiency and viability of pluripotent stem cell-derived human dopaminergic precursors

Shirley D. Wenker[a], Victoria Gradaschi[a,1], Carina Ferrari[a], Maria Isabel Farias[a], Corina Garcia[a], Juan Beauquis[b], Xianmin Zeng[c], Fernando J. Pitossi[a*]

[a]Fundación Instituto Leloir - IIBBA-CONICET, Argentina.

[b]Instituto de Biología y Medicina Experimental, CONICET, Buenos Aires, Argentina; Departamento de Química Biológica, Facultad de Ciencias Exactas y Naturales, Universidad de Buenos Aires, Argentina.

[c] RxCell, CA, USA.

Short title: Functional role of TNF-α on the differentiaton and viability of human dopaminergic neurons

Corresponding author:

Fernando J. Pitossi, Ph.D

Fundación Instituto Leloir- IIBBA CONICET

Av. Patricias Argentinas 435

Ciudad Autónoma de Buenos Aires, CP C1405BWE

República Argentina.

Tel: 54-011-5238-7500

E-mail address: fpitossi@leloir.org.ar

[1]**Present address:** Departamento de Química Biológica. Facultad de Ciencias Exactas y Naturales, Universidad de Buenos Aires (UBA), Argentina.

ABSTRACT

Parkinson ´s Disease is a neurodegenerative disorder characterized by the progressive loss of dopaminergic cells of the *substantia nigra pars compacta*. Even though successful transplantation of dopamine-producing cells into the striatum exhibits favourable effects in animal models and clinical trials; transplanted cell survival is low. Since every transplant elicits an inflammatory response which can affect cell survival and differentiation, we aimed to study *in vivo* and *in vitro* the impact of the pro-inflammatory environment on human dopaminergic precursors. We first observed that transplanted human dopaminergic precursors into the striatum of immunosuppressed rats elicited an early and sustained activation of astroglial and microglial cells after 15 days post-transplant. This long-lasting response was associated with Tumor necrosis factor alpha expression in microglial cells. *In vitro* conditioned media from activated BV2 microglial cells increased cell death, decreased Tyrosine hydroxylase -positive cells and induced morphological alterations on human neural stem cells-derived dopaminergic precursors at two differentiation stages: 19 days and 28 days. Those effects were ameliorated by inhibition of Tumor necrosis factor alpha , a cytokine which was previously detected *in vivo* and in conditioned media from activated BV-2 cells. Our results suggest that a pro-inflammatory environment is sustained after transplantation under immunosuppression, providing a window of opportunity to modify this response to increase transplant survival and differentiation. In addition, our data show that the microglia-derived pro-inflammatory microenvironment has a negative impact on survival and differentiation of dopaminergic precursors. Finally, Tumor necrosis factor alpha plays a key role in these effects, suggesting that this

53 cytokine could be an interesting target to increase the efficacy of human
54 dopaminergic precursors transplantation in Parkinson ´s Disease.

55

Introduction

Neurological disorders are one of the main causes of disability in the world. Among these disorders, Parkinson's disease (PD), affects the second largest group of people and has the highest growth in incidence. From 1990 to 2015, the prevalence of PD and, therefore, disability and cause of death doubled, with a prevalence of 98 cases of PD per 100,000 individuals, representing a 15.7% increase (1).

PD is a neurodegenerative disorder, whose cardinal pathology is the loss of dopaminergic (DA) neurons in the *substantia nigra pars compacta*. Current treatments for PD provide symptomatic relief but have side effects in the long term and do not halt disease progression or regenerate DA cell loss (2).

Cell replacement therapy has been proposed as an alternative strategy due to the fact that motor symptoms of PD are caused by the degeneration of a specific cell type, DA neurons. Therefore, grafts of DA precursors (DAp) could have the potential to replace the function of DAn loss and thus reduce the associated motor symptoms. Pre-clinical and clinical trials have provided proof of concept that the transplantation of DA neuroblasts in the striatum can alleviate parkinsonian symptoms (3,4). DA neuroblasts and not mature DA neurons are used since the transplanted cells need to engraft in the host parenchyma in order to survive. Although the results from clinical trials have demonstrated that this approach is safe, its efficacy was variable and several undesirable side effects such as graft-induced dyskinesia were reported. Thus, standardization of several factors is crucial to optimize the efficiency of the treatment and try to prevent unwanted effects (3,5). One important factor for the development of an effective therapy of cell replacement is the host-primary

response related to the graft. The microenvironment generated by the host could have dramatic effects on the survival, differentiation and proliferation of the transplanted cells. In this context, microglia activation affects dramatically the host environment after a mechanical intervention to the central nervous system (CNS). Cellular transplantation in the CNS not only includes such a mechanical injury but also provides a plethora of inflammatory and immune stimuli to the transplantation site (6). Adaptive immune responses are usually prevented by immunosuppression treatments. However, innate immune responses should remain active after transplantation but scarce information is available on its characteristics, duration and functional effects on the transplant. In particular, the possible effects of microglia, the main effectors of the innate immune response in the brain, on the fate of the transplanted cells are poorly described. Microglial activation produces several pro-inflammatory factors with neurotoxic effects (i.e., Tumor necrosis factor alpha (TNF-α), Interleukin (IL)-1, IFN-gamma, Nitric oxide, and reactive oxygen species) that could compromise the viability and/or differentiation of DA precursors (7). Because grafting to the CNS inevitably causes activation of host's microglia, understanding its functional effects on the viability and differentiation of DA precursors is important in order to detect potential molecular targets to improve the efficacy of cell therapy.

In this work, we found that sustained and increased microglial and astroglial response were observed 15 days post-transplantation even in the presence of a constant immunosuppressive treatment. On the contrary, the transplanted cells elicited only a marginal and transient infiltration of neutrophils. Then, we observed that *in vitro*, activated microglial-derived conditioned media diminished

106 human DAp survival, differentiation and affected cell morphology. These effects
107 were blocked by inhibiting TNF-α in the culture.
108
109 ## Materials and methods
110 ### Reagents
111 All chemicals used were of analytical grade. D-MEM, αMEM; GMEM,
112 Neurobasal, B27, Geltrex, Acutase, penicillin/streptomycin; NEAA; β-
113 mercaptoethanol and KSR were obtained from Gibco. GDNF and BDNF were
114 from Peprotech. L-glutamine; Na pyruvate; dimethylsulfoxide; Mitomicym C;
115 lipopolysaccharide and p-formaldehyde (PFA) were obtained from Sigma-
116 Aldrich. TNF-α -ELISA Kit was obtained from BD. Triton X-100 and Tween 20
117 were from Merck. Fetal bovine serum (FBS), and were obtained from
118 Internegocios SA (Argentina). Cyclosporine was from Novartis.
119
120 ### Cell cultures
121 #### PA6 cells
122 Mouse stromal cell line PA6 (RIKEN BRC) were maintained and propagated
123 αMEM, supplemented with 10% FBS and antibiotics (100 U/ml penicillin, 100
124 μg/ml streptomycin).
125
126 #### Human Neural Stem Cells (hNSCs)
127 hNSCs-H14, kindly gifted by Dr Xianmin Zeng were propagated using
128 Neurobasal medium supplemented with B27, 2 mM NEAA, 20 ng/mL of bFGF
129 and antibiotics (100 U/ml penicillin, 100 μg/ml streptomycin) on Geltrex-coated

dishes. Quality control for hNSCs populations were analyzed by immunofluorescences for Nestin and SOX-1.

Dopaminergic differentiation

Generation of PA6 conditioned media (PA6-CM): PA6 cells were cultured, grown to 80% confluence, and then treated with Mitomycin C (0.01mg/ml; 2 hs). After 5 washes with PBS, PA6 cells were incubated with fresh PA6 culture medium for 16 hs. Then, PA6 maintence culture medium was replaced with ESD medium (GMEM with 10% KSR, 1× NEAA, 1× Na pyruvate, and 1× β-mercaptoethanol). PA6-CM was collected every 24 h during 1 week (8).

DA differentiation was initiated by culturing hNSCs with PA6-CM on culture dishes coated with poly-L-ornithine (20 µg/mL) and laminin (10 µg/mL). After 14 days of differentiation, DA precursors (DA14) (150000 live cells/cm2) were transferred to 24-well plates. Cells were cultured in PA6-CM with BDNF (20 ng/mL) and GDNF (20 ng/mL) until day 28 (DA28) (8).

The different states of maturation from hNSCs cultures to dopaminergic differentiation were analyzed macroscopically and by immunofluorescent staining of differentiation markers such as TH, Foxa-2, TUJ1, GFAP. The characterization was carried out at two stages of the differentiation protocol: day 14 (DA14) and day 28 (DA28) (9).

In vitro treatments were carried out after 24 hs of incubation of DA14 cultures.

BV2 microglial cells

Mouse BV2 microglial cell line was provided by Dr. Guillermo Giambartolomei (Hospital de Clínicas, Buenos Aires, Argentina). Cell line was maintained in 100

mm plastic tissue-culture dishes (GBO) containing D-MEM supplemented with 2 mM L-glutamine, antibiotics (100 U/ml penicillin, 100 μg/ml streptomycin), 10% FBS (10).

All cultures were developed at 37°C with 5% CO_2 and 100% humidity. Media were replaced every 2 days and cells were split before they reached confluence.

Animals

Adult male Wistar rats (Jackson Laboratory, Bar Harbor, ME, USA), bred for several generations in the Leloir Institute Foundation facility, were used in all of the experiments. The animals were housed under controlled temperature conditions (22±2°C), with food and water provided ad libitum and a 12:12 dark:light cycle with lights on at 08.00 h. All experimental procedures involving animals and their care were conducted in full compliance with NIH and internal Institute Foundation Leloir guidelines and were approved by the Institutional Review Board "Cuidado y Uso de Animales de Laboratorio (CICUAL-FIL)". All of the animal groups were periodically monitored, indicating that the welfare of the animals was consistent with the standards of the ethical guidelines for animals.

Cell transplantation

For stereotaxic injections, the animals were anaesthetized with ketamine chlorhydrate (80mg/kg) and xylazine (8mg/kg). Intrastriatal stereotaxic transplantation was conducted on cyclosporine A-immunosuppressed male rats (age: 8 weeks). The stereotaxic coordinates were: bregma +1.0 mm; lateral

+3.0 mm; ventral -5 and –4.5 mm (11). After confirmation of the viability of the hDAp with Trypan blue vital stain, the concentration of the suspension was adjusted to 125000 cell/µL. About 250000 human DAp (viability: 81%) derived from hNSCs-H14 were transplanted into the left striatum by using a Hamilton syringe (12). 2 µl of the cell suspension was inoculated. The injection flow was 0.5µl/min. After injection, the cannula was held in place for 5 min, before being slowly retracted. The experimental animals did not show signs of ongoing disease. They presented with normal fur, activity, movement, and food consumption.

Cyclosporine A (Novartis, 15 mg/kg) was administrated daily (Intraperitoneal injection) until the end of the experiment, starting 2 days before cell transplantation (13).

Host primary response related to the graft were analysed by histological and immunofluorescences techniques at different time points (1, 7, 15 and 28 days. *n*=5 rats per group). In this case, the male rat was the experimental unit.

An aliquot of hDAp obtained from transplantation were cultured for terminal differentiation *in vitro.* At DA28, 17±1% of Tyrosine hydroxylase (TH)-positive cells were detected by immunofluorescence.

In vitro experimental treatments

A) Microglia activation: BV2 cells were seeded in 6-wells plate (75000 cells/cm2). After 24 hs, cell cultures were treated with lipopolysaccharide (LPS) for 24 h according to Dai and collegues (10).

B) DA precursors acute exposure to conditioned media from microglial cells: DA precursors had been previously plated for 24 h, as DA14, in 0.5 ml of PA6

205 medium containing differentiation factors. Activation of BV2 microglial cells (24
206 h) were carried out as explained before. After centrifugation (2000 rpm, 10
207 minutes) 0.6 ml cell-free supernatants (CM, conditioned media) from basal and
208 activated microglial cultures were transferred to wells containing DA precursors
209 (DA15). After 4 days of DA precursor incubation with conditioned medium from
210 BV2 cells (CM-BV2), evaluation of cell survival and differentiation was
211 performed.
212 In TNF-α neutralization experiments etanercept (Enbrel, Pfizer; 100 ng/mL)
213 (14), an inhibitor of both soluble and transmembrane forms of TNF, was added
214 to CM-BV2 as co-treatment.
215

216 **Measurement of nitric oxide**

217 Nitric oxide (NO) production was determined by measuring the accumulation of
218 nitrite, the stable metabolite of NO, in culture medium. Isolated supernatants
219 collected from microglial cell cultures exposed to LPS for the indicated period
220 were mixed with equal volumes of the Griess reagent (1% sulfanilamide, 0,1%
221 naphthylethylenediamine-dihydrochloride, and 2% phosphoric acid) and
222 incubated at 25ºC for 10min. Absorbance at 540 nm was measured in a
223 microplate reader (15).
224

225 **Cytokine quantification**

226 TNF-α was measured by enzyme-linked immunosorbent assay (ELISA) in
227 supernatants obtained as described above for NO measurement. ELISA test
228 was performed according to the manufacturer's instructions of the kit. In each

trial, samples were analyzed in duplicate against standards of known concentration.

Histology

The animals were deeply anaesthetized as previously described (16) and were transcardially perfused with heparinized saline, followed by ice-cold 4% PFA in phosphate buffer (PB) (0,1M; pH 7,2). Brains were dissected and placed in the same fixative overnight at 4°C and cryoprotected in 30% sucrose 0.1M PB solution. Then, the brains were frozen in isopentane and cut using a cryostat into 40-µm serial coronal sections through the left prefrontal cortex. Sections were mounted on gelatine coated slides and stained with Cresyl Violet to assess the general nervous tissue integrity, neutrophils cell counts and inflammation. For immunohistochemistry, sections were stored in cryoprotective solution at −20°C until needed.

Immunofluorescence

Free-floating sections were rinsed in 0.1% Triton in 0,1M PB. After washes with PB-T, samples were blocked in 1% donkey serum for 45 min, and then incubated overnight at 4°C with primary antibodies diluted in blocking solution. The list of antibodies is provided in Table 1. After three 10-minute washes with 0.1 mol/L PB, the sections were incubated with indocarbocyanine (Cy3) or cyanine Cy2 (Cy2)- conjugated donkey anti-rabbit or anti-mouse antibody, respectively (1:500; Jackson ImmunoResearch) for 2 h at room temperature, rinsed in PB and mounted in Mowiol (Calbiochem). Digital images were

obtained in a Zeiss LSM 510 laser scanning confocal microscope equipped with a krypton-argon laser.

Table 1: list of antibodies used

Antibody	Trademark	Catalogue numbers
Anti-GFAP	DAKO	Z0334
Anti-MHCII	Serotec	MCA46G
Anti-ED1	Serotec	MAC341R
Anti-SOX1	R&D system	AF3369
Anti-Nestin	Abcam	ab22035
Anti-TUJ1	Promega	G712A
Anti-MAP-2	Cell Signaling	9043S
Anti-Foxa-2	Abcam	ab117542
Anti- Tyrosine hydroxylase (TH)	Pell-Frezze	P40101
Anti-Caspase 3 active (CA3)	Neuromics	RA15046
Anti-NfkB	SCBT	sc-372
Anti-hNCAM	SCBT	sc-33686
Anti-TNF-α	SCBT	sc-1351

DA cell cultures: samples were fixed with PFA in 4% w/v in PBS, with incubation at room temperature (20 min). After three washes with PBS-T, samples were blocked with 1% donkey serum in PBS-T (1h at room temperature), and then incubated with primary antibody (Table 1), for 16hs at 4°C. After PBS-T washes, incubation with the secondary antibody (1:1000; Jackson ImmunoResearch)

were performed proceed for 2 hrs at room temperature in the dark. At the end, excess antibody was removed with three new washes with PBS, nuclear staining will be performed with Hoechst 33258 dye (1:1000 dilution in PBS). After washing thrice with PBS, samples were mounted in Mowiol (Calbiochem).

BV-2 cells: After fixation with methanol, NFκB immunocytochemistry was performed on BV2 cells to determine nuclear translocation as a proxy for cell activation. Cells attached to coverslips were permeabilized with 0.5% triton X-100 in PBS and unspecific binding sites were blocked with 1% BSA in PBS. Cells were incubated with primary antibody against NFκB and then with Alexa Fluor (488/596; Thermo-Fisher) labeled secondary antibodies. Nuclei were visualized Hoechst 33258 dye (1:1000). After washing thrice with PBS, samples were mounted with Mowiol (Calbiochem).

Fluorescence microscopy: Hoechst nuclear staining of apoptotic cells

DA cell cultures were developed on slide covers plated in in 24-wells plate. After treatments, cells were fixed with PFA 4% w/v in PBS for 20min at 4 °C, exposed to Hoechst 33258 dye in PBS for 30 min at room temperature, and washed thrice with PBS. Finally, samples were mounted and fluorescent nuclei with apoptotic characteristics were detected and analyzed by immunofluorescence microscopy. Apoptotic cells were identified by morphology and nuclear fluorescence intensity. The condensed chromatin within apoptotic cells stains particularly heavily showing blue fluorescense. In addition, little apoptotic bodies released from nuclei are also detected because of their brilliant blue color. Differential cell count was performed by evaluating at least 1000 cells (15).

Images were captured with Zeiss Axio Observer and Zeiss LSM 510 laser scanning confocal microscope equipped with a krypton-argon laser.

Image analysis

Polymorphonuclear-neutrophil (PMN) cells were identified by their nuclear morphology appearance in 40-µm thick cresyl violet-stained sections. For MHC II-positive and GFAP-positive cell quantification, approximately 10 fields were quantified for each animal using the Zeiss Image J software. The total number of positive cells was normalized to the total area counted for each sample (16). Twenty images were obtained by random sample and the analysis was performed using the Image J software. Using the image overlay and cell count plugings, the total number of cells per field and the number of cells positive for the corresponding labeling were counted (example: TH, TUJ1, Foxa-2). In this way, the percentage of positive cells will be obtained in relation to the number of nuclei counted. At least 1000 total cells were counted.

Differentiation analysis

DA precursors were seeded and after 24 h-incubation, DA15 were exposed to CM-BV2. Cell morphology was observed under phase-contrast in an inverted microscope at 200x magnification and photographed by using a Nikon DS-L3 digital camera. Cell differentiation was determined in independent experiments by counting differentiated cells based on morphological criteria (17) and expressed as percentage of total cells (at least 500 cells).

For neurite outgrowth analysis from TH+ cells derived from DA differentiation were performed at DA19 and DA28 stages. Multiple independent images were

taken from immunofluorescence against TH at 400x magnification. At least 10 neurites per field were selected for neurite outgrowth measurement and means of neurite length were calculated for each assay. This neurite tracing technique was implemented in the form of a plugin (NeuronJ) for ImageJ, the computer-platform independent public domain image analysis program inspired by NIH-Image (18).

Statistical analysis

Statistical analysis was performed using GraphPad Prism, version 6.00 for Windows (GraphPad Software, San Diego, CA, USA). Results were expressed as mean and standard error (SEM) of n independent trials (at least 3) indicated in each figure. Statistical significance was calculated using two-tailed Student's t test or ANOVA followed by *post hoc* multiple comparison test as indicated. When corresponding statistical differences between groups were assessed by means of the Mann-Whitney test or the Kruskal-Wallis One Way Analysis of Variance. At least differences with $P<0.05$ were considered the criterion of statistical significance.

Results

Host response to hDAp transplantation

hNSCs expressed over 95% of Nestin and Sox-1, proving that they were *bona fide* hNSC (Fig. 1C). Human dopaminergic precursors (hDAp) were obtained by incubating hNSCs with PA6-conditioned medium (PA6-CM) (Fig.1A). We observed morphological changes such as outgrowth of elongated cells (Fig. 1B). After 14 days, DA precursors (DA14) expressed characteristic early DA

338 markers such as Foxa-2 (72,6±4,7 %) and late markers such as Tyrosine
339 hydroxylase (TH) (5,5±0,8 %). By 28 days, an increase in neuron-like cells was
340 observed. As expected for such a protocol, at 28 days, cultures contained
341 approximately 19,1±0,9% TH-positive cells; 70,5±7,3 % positive cells for the
342 pan-neuronal marker, TUJ1; and less than 5 % of glial cells (3,4±0,5 % GFAP-
343 positive cells) (Fig.1C).
344
345 **Fig 1. Dopaminergic differentiation from hNSCs.**
346 (A) Differentiation protocol was initiated by culturing hNSCs-H14, in PA6-CM for
347 14 days (DA14). After this period, PA6-CM was supplemented with rhBDNF and
348 rhGDNF for a period of 14 days (DA28). (B). Photographs from each stage
349 shown morphological changes. (C) Quality control for hNSCs populations were
350 analyzed by immunofluorescence technique for Nestin and SOX-1. Different
351 stages of maturation from cultures of hNSCs induced to dopaminergic
352 differentiation were analyzed by immunofluorescence. The expression of the
353 following markers were detected and quantified at two stages of the
354 differentiation protocol: Foxa-2 and TH for DA14 cells (DA precursors) and
355 TUJI; GFAP and TH for DA28. Cell nuclei were labelled by Hoechst staining.
356 Each bar represents mean±SEM of independent assays. Magnification: 40X.
357
358 A preparation of 250.000 hDAp with at least 80% living cells was trasplanted
359 into the striatum of cyclosporine A-daily immunosuppressed rats during 28 days
360 (Fig. 2A) (12). Post-mortem evaluation revealed surviving grafts, visualised by
361 the presence of human-specific NCAM staining (Fig.2B).
362

Fig 2: Primary host response related to the graft.

(A) DA14 cells were obtained from hNSCs and 250000 cells (viability: 81%) were transplanted into the striatum of immunosuppressed Wistar male rats (age: 8 weeks). At different time points (1, 7, 15 and 28 days) host primary response related to the graft were analysed by immunofluorescences technique. (B) Detection of human-specific NCAM (hNCAM) allowed for identification of the graft. (D) Astrocytes (GFAP-positive cells) and activated microglia (MHCII-positive cells) related to the graft can be observed after 7 days of surgery. (E-F) There is a significant increase in MHCII+ and GFAP+ cells at 15 and 28 days post graftment of hDA14 (*p<0,05 and **P<0.01). Kruskal-Wallis ANOVA followed by Dunn`s post hoc test, n=5. (G) Finally expression of TNF-α were observed at Day 28 post surgery. Representative pictures of the grafts are shown (Magnification: 40X). Each bar represents mean±SEM of independent assays

Histological analysis revealed an early neutrophil infiltration (1day: 4,04e-4±8.50e-5 Neutrophils/area) from the periphery, which was resolved by 7 days (5,46e-5±2,25e-5 Neutrophils/area. *p<0,05 vs. 1 day) (Fig. 2C). Astroglial activation as seen by GFAP-staining, increased 7 days after transplantation, reaching a peak at 15 days (1 day: 2,13e-4±2,54e-5 vs. 15 days: 9,76e-4±1,03e-4 GFAP+cells/area. **p<0.01), beginning to decay at 28 days (28 days: 8,34e-4±9,58e-5 GFAP+cells/area. *p<0,05 vs. 1 day) (Fig. 2D, 2E). Transplantation of hDAp in cyclosporine A-daily immunosuppressed rats resulted in microglial activation as demonstrated by the presence of MHC-II+ cells, which specifically label activated microglia (16,19). MHC-II stained all the

activation stages but not resting microglia. According to our results, MHC-II+ cells presented the typical morphology of activated microglial cells: elongated-shaped cell body with long and thicker processes and/o round-shaped body with short, thick and stout processes (Fig. 2 D). Statistical analysis of microglial activation determined by MHCII-positive cell density showed a marked increase at 15 days (1 day: 6,67e-5±1,32e-5 vs. 15 days: 2,19e-4±1,96e-5 MHCII+cells/area. *p<0,05) which was sustained up to the last time point analysed 28 days: 3,29e-4±2,16e-5 MHCII+cells/area. **p<0.01 vs. 1 day) (Fig.2D, 2F).

Interestingly, tumor necrosis factor alpha (TNF-α) expression was detected 28 days post-surgery in ED1-positive microglial cells within the graft core and the periphery (Fig. 2G). These results show that there is a sustained host response to the transplant in immunosuppressed animals.

Conditoned media from microglia have toxic effects on hDAp: short term effects

Previously, we observed a primary response related to the xenograft of hDAp, with a significantly increase of microglial activation. As the effects of the host microglial cells on the fate of the transplanted dopaminergic precursors are poorly described, we were interested in simulate the impact of rodent microglial activation on the differentiation and survival of hDAp derived from NSCs.

Microglial activation using bacterial lipopolysaccharide (LPS), was analysed by determining pro-inflammatory mediators such as nitrites (NO) and TNF-α in the cell culture supernatant. LPS led to a significant increase in nitrite production (Basal: 1,2±0,7 vs. Activated (LPS): 31,9±1,5 uM. **P<0.01) and TNF-α

413 secretion (Basal: 22,3±14,3 vs. Activated (LPS): 739,7±76,1 pg/ml. *P<0.05) 24
414 h after cell activation (Fig. 3A, 3B). In addition, NFkB nuclear translocation was
415 also observed in BV2 cell cultures after cell activation (Fig. 3C).
416
417 **Fig 3: Characterization of microglial cell activation.**
418 BV2 cultures were exposed or not (Basal) to LPS (Activated), and parameters
419 of microglial cell activation were determined. (A) Nitrite production (Griess
420 method) and TNF-α secretion (ELISA test) (B) were measured after 24 h of cell
421 activation. (C) NFkB nuclear translocation was analyses by
422 immunofluorescences after short term exposure to LPS. Significant increases in
423 nitrite and TNF-α were induced by LPS treatment. Asterisks indicate statistically
424 significant differences: nitrite, **P<0.01 with respect to basal condition (n=5) and
425 *P<0.05 TNF-α with respect to basal condition (n=5) (Mann-Whitney test).
426 Microscopy images of NFκB-stained microglia under basal conditions or
427 activated after LPS treatment (Magnification: 40X). Values are means±SEM of n
428 independent trials.
429
430 In order to analyze the short-term effect of microglial activation on hDAp, we
431 exposed DA15 cultures to conditioned medium from BV2 cells (basal –CM-BV2
432 Basal- or activated condition –CM-BV2 Activated-) until DA19 (Fig. 4A).
433 Morphological analysis were performed. A decrease in neuron-like cell count
434 (CM-BV2 Basal: 72,8±1,9 vs. CM-BV2 Activated: 57,9±2,4 %.***p<0,001. Figure
435 4B,4C) and neurite length of TH positive cells was detected in DA precursors
436 cultures incubated with CM from activated microglia (CM-BV2 Basal:
437 339,0±31,2 vs. CM-BV2 Activated: 148,0±15,4 neurites lenght.***p<0,001) (Fig.

438 4B-E). A significant reduction of TH-immunoreactive cells was detected in DA
439 cultures exposed to CM from activated BV2 compared to basal conditions (CM-
440 BV2 Basal: 5,9±0,4 vs. CM-BV2 Activated: 2,5±0,4 %TH+cells. ***p<0,001. Fig.
441 4F, 4G). Concomitant with these results, we observed an increment in apoptotic
442 nuclei (CM-BV2 Basal: 7,2±0,7 vs. CM-BV2 Activated: 21,4±2,5 % apoptotic
443 cells. **p<0,01. Fig. 4I) and caspase activated 3 (CA3)-positive cells (Fig. 4H) in
444 DA precursors after 4 days of incubation with CM from activated microglia.
445
446 **Fig 4. Effect of the activated microglia CM in the differentiation of DA**
447 **precursors.**
448 (A) DA15 cultures were exposed to microglia CM (Basal or Activated) until day
449 19 (DA19). (B-E) For semi-quantitative analysis, photographs from independent
450 experiments were analyzed to determine neuron-like cell count and neurites
451 length. Asterisks indicate statistically differences (***p<0.001. Unpaired T-test.
452 n=7) in percentage of neural-cell-like (C) and neurite length (E) of DA
453 precursors cultured under inflammatory conditions (CM-BV2 activated) versus
454 basal (CM-BV2 basal). There is a decrease in the number of cells with neuronal
455 morphology and neurite length in DA precursors exposed with CM-BV2
456 activated. (F) Confocal images of TH-stained DA19 cell cultures. G) Asterisks
457 indicate statistically differences (***p<0.001. Unpaired T-test. n=9) for cell
458 counting assays of TH+ cells of DA precursors cultured with CM-BV2 activated
459 versus basal (CM-BV2 basal). (H-I) Cell death was analyzed by fluorescence
460 microscopy using Hoechst and detection of activated caspase 3 (CA3) by
461 immunofluorescence. (H) Arrowheads indicate apoptotic nucleus and CA3-
462 immunoreactive cell. An increment of CA3-positive cells (see indicator arrows)

463 was observed in DA precursors incubated with CM-BV2 activated (40x
464 magnification). (I) Asterisks show statistically significant differences (**p<0.01.
465 Mann Whitney. n=6) in DA precursors incubated with CM-BV2 activated versus
466 CM-BV2 basal. Values are means±SEM for the percentage of apoptotic cells
467 relative to the total cell number.
468
469 **Conditoned media from microglia have toxic effects on hDAp: long term**
470 **effects**
471 In order to know if the short term effects after acute exposure to inflammatory
472 conditions were transient or not, the protocol described before were carried out
473 until DA19. Then, cell medium was replaced with PA6-CM (DA differentiation
474 medium) and then, at the final stage of DA differentiation protocol (DA28),
475 survival and morphological parameters were studied (Fig. 5A). At DA28, a
476 statistical reduction in the percentage of neuronal-like cells (CM-BV2 Basal:
477 89,6±2,9 vs. CM-BV2 Act: 64,5±3,9 %. ***p<0,001) and neurite length (CM-
478 BV2 Basal: 383,6±24,9 vs. CM-BV2 Act: 183,5±24,1. ***p<0,001) were detected
479 in those cultures who were exposed for an acute period of time to a microglial
480 activated-environment (CM-BV2 Activated) (Fig. 5B-E). Moreover, a reduction in
481 the percentage of TUJ1-positive cells, in cell cultures exposed with CM-BV2
482 Activated was obseved (CM-BV2 Basal: 54,0±3,1 vs. CM-BV2 Act: 29,8±0,9
483 %TUJ1+cells. ***p<0,001) (Fig. 8C, 8E). In addition, our results showed
484 significant decrease in the percentage of TH-positive cells in DA cultures
485 treated with CM from activated BV2 (CM-BV2 Basal: 9,8±0,5 vs. CM-BV2 Act:
486 4,3±0,5 %TH+cells. ***p<0,001) (Fig. 5F, 5G). We conclude that there is no

487 recovery of TH-positive cells in cultures initially incubated under inflammatory
488 conditions.
489
490 **Fig 5. Impact of pro-inflammatory microenvironment on DA cultures.**
491 (A) CM from basal and activated condition were added to DA precursors and
492 incubated during 4 days. Morphological analysis and detection of DA neurons
493 were performed at DA28. (B-E) For semi-quantitative analysis, photographs
494 from independent experiments were analyzed to study morphological alterations
495 and determine neuron-like cell count and neurites length. Asterisks indicate
496 statistically significant differences at DA28 stage (***p<0.001. Unpaired T-test.
497 n=6) in the percentage of neural-cell-like (C) and neurite length of TH-positive
498 cells (***p<0.001. Unpaired T-test. n=6) (E) of hDAp cells cultured under
499 inflammatory conditions (CM-BV2 activated) versus basal (CM-BV2 basal). (F-
500 G) Cell counting of TH-positive cells was performed. Representative
501 photomicrographs from TH immunofluorescence (40x) of DA28 cells obtained
502 from DA28 cultured with CM-BV-2 (basal and activated condition) are shown.
503 Asterisks indicate statistically significant differences (***p<0.001. Unpaired T-
504 test. n=6) for cell counting assays of TH+ cells of hDAp cultured under
505 inflammatory conditions (CM-BV2 activated) versus basal microenvironment
506 (CM-BV2 Basal) (G). Values are means±SEM of n independent trials.
507
508 **Functional effects of TNF-α on survival and differentiation of DA**
509 **precursors**
510 Previously, the pro-inflammatory cytokine TNF-α was observed to be expressed
511 after transplantation (Fig. 2G), which was detected in cell culture supernadant of

512 activated microglia (Fig. 3B). Earlier studies reported citotoxic effects of TNF-α
513 in neural cell lines (20). These findings lead us to study the role of TNF-α in the
514 differentiation and survival of hDAp.
515 DA15 were cultured with CM-BV2 (basal or activated condition) during 4 days
516 as previously described, with or without Etanercept (a TNF-α inhibitor) as co-
517 treatment (Fig. 6A). Neuronal differentiation was analysed by cell morphology
518 and TUJ1-cell counting. Acute exposure to CM from activated microglia (CM-
519 BV2 Act) affected cell morphology and TUJ1-positive cell percentage (CM-BV2
520 Basal: 43,9±1,4 vs. CM-BV2 Act: 30,3±1,4 %TUJ1+cell. ***p<0,001), while
521 TNF-α blockage was able to reverse neuronal loss (CM-BV2 Act+Etan:
522 40,9±1,7 vs. CM-BV2 Act: 30,3±1,4 %TUJ1+cell. **p<0,01) (Fig. 6B-E).
523
524 **Fig 6. Effect of TNF-α inhibitor on differentiation of DA precursors**
525 **exposed to activated microglia CM.**
526 (A) DA precursors were exposed with CM-BV2 during the 4 days, in the
527 presence of Etanercept (a TNF-α inhibitor). (B) For semi-quantitative analysis,
528 photographs from independent experiments were analyzed to determine
529 neuron-like cell count. (C) Detection of TUJI+ cells by immunofluorescence and
530 cell counting were performed at DA19. Photomicrographs are shown (40x). (D)
531 Asterisks indicate statistically significant differences in percentage of neural-cell
532 like DA precursors cultured under inflammatory conditions (CM-BV2 activated)
533 versus basal (CM-BV2 basal) (*p<0.01 CM-BV2 Act vs. CM-BV2 Basal).
534 Inhibition of TNF-α prevents the decrease in the number of cells with neuronal
535 morphology (*p<0.05 CM-BV2 Act vs. CM-BV2 Act+Etan). ANOVA followed by
536 Tukey`s post hoc test. n=4 independent assays. (E) Asterisks indicate

537 statistically significant differences in percentages of TUJI+ cells of hDAp
538 cultured with CM from activated BV2 cultures versus CM from BV2 cells under
539 basal conditions (***p<0.001 CM-BV2 Act vs. CM-BV2 Basal). Co-incubation of
540 hDAp with Etanercept inhibited TUJI+ cells diminution (**p<0.01 CM-BV2 Act
541 vs. CM-BV2 Act+Etan). ANOVA followed by Bonferroni test. n=5 independent
542 assays. Values are means ± SEM of n independent trials.
543
544 In addition, Etanercept had no effects on the expression of TH when hDAp were
545 incubated with CM from basal BV2 cells. However, inflammatory-mediated
546 suppression of TH expression was overtly reversed by Etanercept co-treatment
547 (CM-BV2 Act+Etan: 5,7±0,5 vs. CM-BV2 Act: 2,6±0,5 %TH+cells. **p<0,01)
548 (Fig.7B, 7E). Quantification of neurite length of DA19 indicated that, while pro-
549 inflammatory conditions caused a decrease in neurite length, co-treatment with
550 Etanercept reduced these alterations in TH-positive cells (Fig. 7C, 7D). Finally,
551 we measured cell death in DA19. Our results suggest that TNF-α mediated
552 inhibition partially reduced the percentage of apoptotic cells (Fig. 7F).
553
554 **Fig 7. Effect of TNF-α inhibitor on survival and neurite length of DA**
555 **precursors exposed to inflammatory conditions.**
556 (A) DA precursors were cultured in the presence of CM-BV2 (basal or activated
557 condition) during 4 days, in the presence of Etanercept as co-treatment. (B)
558 Detection of TH+cells by immunofluorescence and cell counting were
559 performed at DA19. Photomicrographs from immunofluorescence are shown
560 (40x). (C) Neurite length analyzes of TH+ cells were also performed at DA19.
561 Photomicrographs are shown (40x). (D) Decrease in neurite length were

562 observed after exposure of DA precursors to activated CM-BV2 (**p<0.01 vs.
563 CM-BV2 Basal). Inhibition of TNF-α reduces alterations in neurite length of TH+
564 cells (**p<0.01 CM-BV2 Act vs. CM-BV2 Act+Etanercept). ANOVA followed by
565 Bonferroni test. n=4. (E) Exposure of DA precursors to activated CM-BV2
566 decreased the percentage of TH+ cells (*** p <0.001 vs. CM-BV2 Basal).
567 Inhibition of TNF-α prevents TH+ cell loss (**p<0.01 CM-BV2 Act vs. CM-BV2
568 Act+Etan. ANOVA followed by Bonferroni test. n=7). (F) Cell death was
569 analyzed by apoptotic nucleus counting after Hoechst staining. The results
570 showed that exposure of DA precursors to CM- from activated microglia
571 significantly increase in cell death (*p<0.05 vs. CM-BV2 Basal. Kruskal-Wallis
572 test ANOVA followed by Dunn`s test. n=7). Partial reduction of apoptotic cells
573 are detected in cell culture treated with Etanercept. Values are means±SEM of
574 n independent trials.
575
576 Similar effects of TNF-α inhibition were observed in all parameters studied
577 previously at the terminal differentiation stage (DA28), suggesting a persistant
578 protection of the hDAp after Etanercept treatment (Fig. 8 and 9).
579
580 **Fig 8. Inhibition of TNF-α and final differentiation of DA precursors**
581 **exposed to proinflammatory conditions.**
582 (A) DA precursors were exposed with CM-BV2 (basal or activated condition)
583 during the 4 days, in the presence of Etanercept. At DA19, cell media was
584 changed to PA6-CM. Morphological assay and detection of TUJI+ cells by
585 immunofluorescence were performed at DA28. (B, D) For semi-quantitative
586 analysis, photographs from independent experiments were analyzed to

587 determine neuron-like cell count. Asterisks indicate statistically significant
588 differences in percentage of neural-cell-like of DA precursors cultured under
589 inflammatory conditions (CM-BV2 activated) versus basal (CM-BV2 basal)
590 (**p<0.01 CM-BV2 Act vs. CM-BV2 Basal). Inhibition of TNF-α prevents the
591 decrease in the number of cells with neuronal morphology (*p<0.05 CM-BV2
592 Act vs. CM-BV2 Act+Etan). ANOVA followed by Tukey`s post hoc test. n=4. (C,
593 E) Photomicrographs from TUJ1 immunofluorescese (40x) of DA28 cultures are
594 shown. Asterisks indicate statistically significant differences in percentages of
595 TUJ1+ cells of DA cultures exposed with CM from activated BV2 cultures
596 versus CM from BV2 cells under basal conditions (***p<0.001 CM-BV2 Act vs.
597 CM-BV2 Basal). Co-incubation of DA cell cultures with Etanercept inhibited
598 TUJI+ cells diminution (**p<0.01 CM-BV2 Act vs. CM-BV2 Act+Etan.) (n=7
599 independent assays). ANOVA followed by Bonferroni test. Values are
600 means±SEM of n independent trials.
601
602 **Fig 9. Long term study of Etanercept effect on DA cultures exposed to**
603 **acute inflammatory conditions.**
604 (A) DA precursors were cultured in the presence of CM-BV2 (basal or activated
605 condition) during the 4 days. A co-treatment of DA precursors with CM-BV2 and
606 Etanercept were performed. (B-C) At DA28, immunofluorescence agaisnt the
607 dopaminergic marker TH and neurite length analyzes were performed. Cell
608 death was analyzed by apoptotic nucleus counting after Hoechst staining.
609 Photomicrographs from immunofluorescence are shown (40x). (D) Diminution in
610 neurite length were observed in DA cultures incubated to CM from activated
611 BV2 (***p<0.001 CM-BV2 Act vs. CM-BV2 Basal). Inhibition of TNF-α reduces

612 alterations in neurite length of DA cells (**p<0.01 CM-BV2 Act vs. CM-BV2
613 Act+Etan. ANOVA followed by Bonferroni test. n=6)). E) Acute exposure of DA
614 precursors to CM from activated microglia decreased the final percentage of
615 TH+ cells (***p<0.001 CM-BV2 Act vs. CM-BV2 Basal). Etanercept co-
616 incubation was able to prevent TH+ cell loss (***p<0.001 CM-BV2 Act vs. CM-
617 BV2 Act+Etan. ANOVA followed by Bonferroni test). (F) The results from cell
618 death analyses show that acute exposure of DA precursors to CM- from
619 activated microglia increase in cell death (*p<0.05 vs. CM-BV2 Basal. Kruskal-
620 Wallis test ANOVA followed by Dunn`s test. n=7). Etanercept was able to
621 reduce the percentage of apoptotic cells. Values are means±SEM of n
622 independent trials.
623

624 **Discussion**

625 Cell replacement therapy involves disruption of the blood–brain barrier (BBB)
626 and host tissue damage, which cause astrocyte and microglia activation
627 (21,22). Therefore, grafted cells are surrounded by an altered environment
628 where host tissue signals could affect relevant processes for the efficacy of cell
629 therapy, such as survival and differentiation of DA precursors.

630 In this study, we have investigated for the first time the short-term response of
631 the cerebral parenchyma to human DA precursors (hDAp) transplantation and
632 further studied the effects of the microglia response on hDAp viability and
633 differentiation *in vitro*. We show that a glial response was sustained in time after
634 transplantation, together with TNF-α expression, under immunosuppression
635 conditions. *In vitro*, acute exposure to conditioned media (CM) from activated
636 microglia diminished the percentage of TH positive cells, induced cell death and

637 affected the differentiation process. In addition, this acute pro-inflammatory
638 treatment of hDAp had a negative impact on terminal differentiation. Finally,
639 specific inhibition of TNF-α reduced the loss of hDAp and the alterations in
640 morphology.

641 In our *in vivo* model, a short-term host primary response related to the grafted
642 hDAp (DA14) was detected with a significant increase of host MHCII- and
643 GFAP-positive cells in adult immunosuppresed male rats. These observations
644 were supported using other cell types who demonstrated an early increase in
645 Iba1- and GFAP-positive cells following a NSC graft, until day 3 post-surgery
646 (22). Further support to our observations come from work by Tomov and
647 colleges who observed microglia and GFAP-positive cells between 7 and 28
648 days after allogeneic transplantation of ventral mesencephalic (VM) cells in a
649 rodent model of PD (6,23). In addition, MHCII-positive cells around hDAp grafts
650 derived from iPSCs were detected long-term in a PD model of
651 immunosuppressed non-human primates (24). At the molecular level, we
652 observed expression of the pro-inflammatory cytokine TNF-α in host-microglia
653 (ED-1)-positive cells after transplantion with hDAp. Interestingly, TNF-α was
654 also detected on the acute period following VM neuroblasts allogeneic grafts
655 from rodents (25) and in allogeneic and xenogeneic transplantation of VM
656 neuroblasts from rodents and pig, respectively (26). Therefore, our data extend
657 and support previous observations on an early host response after brain
658 grafting of other cell types and animal models. Taken together, we preliminary
659 conclude that there seems to be no overt specificity on the host innate immune
660 response to different transplanted cell types at the cellular level.

We also developed an *in vitro* approach which partially simulates the pro-inflammatory microenvironment from the host response related to the graft. This system is based on exposure of hDAp derived from human NSCs to conditioned media from activated BV-2 microglial cells at short-(DA19) and long-term (DA28) end points. Previous research has demonstrated that BV2 cells are a valid model of primary microglia culture (27). In addition, rodent TNF can activate human TNFRI and TNFRII (28). Other microglial models such as primary microglial cultures or human iPSC-derived microglia could be used in future experiments to test similar hypotheses as in this work.

Our results showed a significant increase in cell death of DA precursors exposed with CM from activated microglia by means of a decrease in TH-positive cells in early and late cell culture stages. Our data on cell death extend similar effects of CM from activated microglia observed in other cell types such as SH-SY5Y and PC12 cultures (10,15). Previous reports suggest that the crosstalk between the Bcl family and NF-κB could be involved in DAn vulnerability (29,30). The functional role of these molecules required further analyses.

We also observed morphological alterations specifically induced by CM from activated microglia, such as a decrease in neuron-like cells and neurite length of TH-positive cells at both stages of DA differentiation. Moreover, the percentage of TUJ1-positive cells, a pan-neuronal marker, was diminished by microglia activation. Interestingly, using human cortical neural progenitor cells, TNF-α treatment during six days reduced TUJ1 percentage and increase GFAP-positive cells, suggesting that this cytokine inhibited neuronal differentiation (31). Altogether, our results and others indicate that activated

686 microglial cells and TNF-α could play a role in the survival and differentiation of
687 hDAp and other cells after transplantation.
688 From the evidence obtained *in vivo*, we were interested in analyzing the effect
689 of TNF-α on hDAp. Co-treatment of activated CM with Etanercept, a TNF-α
690 inhibitor, was able to reverse the reduction of TH-positive cells, cell death and
691 morphological alterations previously observed in hDAp. These results extend a
692 previous finding which reported that inhibition of TNF-α reversed the reduction
693 of DA markers and morphological alterations in other cells such as human TH-
694 positive cells derived from Synovial adipose stem cells (32).
695 As we mentioned above, none of the current PD therapies stops
696 neurodegeneration or functionally replaces dopaminergic neuronal loss.
697 Currently, a remarkable effort is being made in order to take cell replacement
698 therapy for PD to the clinic (5). Recently, in 2018, the first clinical trial using
699 GMP-grade hDAp derived from iPSCs was launched, a case report of
700 autologous-cell therapy for PD was published last year and a phase 1 study
701 to evaluate pluripotent stem cell-derived hDAp in patients with PD was
702 approved by the regulatory authorities of US (33,34). Survival, differentiation
703 and integration of the transplanted precursors are biological processes that
704 could influence the effectiveness of this strategy and are affected by the host
705 response (21).
706 In particular, a major limiting factor of cell replacement therapy for PD is still the
707 poor survival rate (10%) of grafted DA precursors (35). Our study points to TNF-
708 α inhibition as a possible strategy to increase survival and differentiation of
709 grafted hDAp. It remains to be determined whether the sole inhibition of TNF or
710 any of its receptors after transplantation is necessary and sufficient to inhibit the

711 deleterious effects of inflammation as we have observed *in vitro*. Nevertheless,
712 several TNF-α inhibitors are clinically available for other diseases. A possible
713 strategy that could be used is the transplantation of DA precursors along with
714 co-infusion of a TNF inhibitor or monoclonal antibodies since inhibitors against
715 TNF-α such as Etanercept and TNF-R1 antagonist as ATROSAB cannot cross
716 BBB under physiological conditions. Alternatively, since cell transplantation
717 include temporal BBB disruption, treatment with agents to neutralize TNF-α
718 deleterious action could be used immediately after surgery. On the other hand,
719 the peripheral administration of a soluble TNF-α inhibitor (XPro1595) was
720 neuroprotective on an *in vivo* model of PD (36). Then, molecules such as
721 XPro1595 could be good candidates to be used in animals models of cell
722 replacement therapy for PD in order to analyze its potential in this specific
723 strategy.
724 In conclusion, our data indicate that microglia-derived TNF-α plays a key role in
725 the possible effects of the host response to hDAp transplantation by affecting
726 survival and differentiaton at short and long-term. Selective targeting of TNF-α
727 holds translational potential to increase survival and differentiation of DA
728 precursors even under immune suppressive treatments targetting the adaptive
729 immune response. Finally, the *in vitro* model described might be useful to study
730 the mechanism of action of microglia on hDAp and search for potentials anti-
731 inflammatory and/or neuroprotective treatments in order to improve survival and
732 differentiation efficacy of hDAp.
733

Author Contributions

Conceptualization: FJP. Investigation and Methodology: SDW, VG, CG, MIF, JB. Formal Analysis: SDW, FJP. Project Administration: SDW, FJP. Funding Acquisition: FJP, SDW. Writing – Original Draft Preparation: SDW, FJP. Writing – Review & Editing: CF, CG. SDW, CF, CG, JB, FJP are members of the research career of CONICET. MIF is member of the MTA career of CONICET.

References

1. Dorsey ER, Bloem BR. The Parkinson Pandemic—A Call to Action. JAMA Neurol. 2018 Jan 1;75(1).
2. Coelho M, Ferreira JJ. Late-stage Parkinson disease. Nat Rev Neurol. 2012 Aug 10;8(8).
3. Wenker SD, Leal MC, Farías MI, Zeng X, Pitossi FJ. Cell therapy for Parkinson′s disease: Functional role of the host immune response on survival and differentiation of dopaminergic neuroblasts. Brain Res. 2016 May;1638.
4. Brundin P, Strecker RE, Widner H, Clarke DJ, Nilsson OG, Astedt B, et al. Human fetal dopamine neurons grafted in a rat model of Parkinson's disease: immunological aspects, spontaneous and drug-induced behaviour, and dopamine release. Exp Brain Res. 1988;70(1):192–208.
5. Parmar M, Grealish S, Henchcliffe C. The future of stem cell therapies for Parkinson disease. Nat Rev Neurosci. 2020 Feb 6;21(2).
6. Tomov N, Surchev L, Wiedenmann C, Döbrössy MD, Nikkhah G. Astrogliosis has Different Dynamics after Cell Transplantation and Mechanical Impact in the Rodent Model of Parkinson's Disease. Balkan

759 Med J. 2018 Mar 15;35(2).

760 7. Hassanzadeh K, Rahimmi A. Oxidative stress and neuroinflammation in
761 the story of Parkinson's disease: Could targeting these pathways write a
762 good ending? J Cell Physiol. 2019 Jan;234(1).

763 8. Peng J, Liu Q, Rao MS, Zeng X. Using Human Pluripotent Stem Cell–
764 Derived Dopaminergic Neurons to Evaluate Candidate Parkinson's
765 Disease Therapeutic Agents in MPP $^{+}$ and Rotenone Models. J Biomol
766 Screen. 2013 Jun 30;18(5).

767 9. Liu Q, Pedersen OZ, Peng J, Couture LA, Rao MS, Zeng X. Optimizing
768 dopaminergic differentiation of pluripotent stem cells for the manufacture
769 of dopaminergic neurons for transplantation. Cytotherapy. 2013
770 Aug;15(8).

771 10. Dai X, Li N, Yu L, Chen Z, Hua R, Qin X, et al. Activation of BV2 microglia
772 by lipopolysaccharide triggers an inflammatory reaction in PC12 cell
773 apoptosis through a toll-like receptor 4-dependent pathway. Cell Stress
774 Chaperones. 2015 Mar 12;20(2).

775 11. Paxinos G, Watson C. The rat brain in stereotaxic coordinates. Orlando,
776 FL: Academic Press; 1986.

777 12. Brüstle O, Cunningham MG, Tabar V, Studer L. Experimental
778 Transplantation in the Embryonic, Neonatal, and Adult Mammalian Brain.
779 Curr Protoc Neurosci. 1997 Nov;1(1).

780 13. Jensen MB, Krishnaney-Davison R, Cohen LK, Zhang S-C. Injected
781 Versus Oral Cyclosporine for Human Neural Progenitor Grafting in Rats. J
782 Stem Cell Res Ther. 2012;01(S10).

783 14. Papazian I, Kyrargyri V, Evangelidou M, Voulgari-Kokota A, Probert L.

Mesenchymal Stem Cell Protection of Neurons against Glutamate Excitotoxicity Involves Reduction of NMDA-Triggered Calcium Responses and Surface GluR1, and Is Partly Mediated by TNF. Int J Mol Sci. 2018 Feb 25;19(3).

15. Wenker SD, Chamorro ME, Vittori DC, Nesse AB. Protective action of erythropoietin on neuronal damage induced by activated microglia. FEBS J. 2013 Apr;280(7).

16. Silva BA, Leal MC, Farías MI, Avalos JC, Besada CH, Pitossi FJ, et al. A new focal model resembling features of cortical pathology of the progressive forms of multiple sclerosis: Influence of innate immunity. Brain Behav Immun. 2018 Mar;69.

17. López-Carballo G, Moreno L, Masiá S, Pérez P, Barettino D. Activation of the Phosphatidylinositol 3-Kinase/Akt Signaling Pathway by Retinoic Acid Is Required for Neural Differentiation of SH-SY5Y Human Neuroblastoma Cells. J Biol Chem. 2002 Jul;277(28).

18. Bonafina A, Fontanet PA, Paratcha G, Ledda F. GDNF/GFRα1 Complex Abrogates Self-Renewing Activity of Cortical Neural Precursors Inducing Their Differentiation. Stem Cell Reports. 2018 Mar;10(3).

19. Pott Godoy MC, Ferrari CC, Pitossi FJ. Nigral neurodegeneration triggered by striatal AdIL-1 administration can be exacerbated by systemic IL-1 expression. J Neuroimmunol. 2010;222(1–2).

20. Pregi N, Wenker S, Vittori D, Leirós CP, Nesse A. TNF-alpha-induced apoptosis is prevented by erythropoietin treatment on SH-SY5Y cells. Exp Cell Res. 2009 Feb;315(3).

21. Salado-Manzano C, Perpiña U, Straccia M, Molina-Ruiz FJ, Cozzi E,

809 Rosser AE, et al. Is the Immunological Response a Bottleneck for Cell
810 Therapy in Neurodegenerative Diseases? Front Cell Neurosci. 2020 Aug
811 11;14.
812 22. Hoornaert CJ, Le Blon D, Quarta A, Daans J, Goossens H, Berneman Z,
813 et al. Concise Review: Innate and Adaptive Immune Recognition of
814 Allogeneic and Xenogeneic Cell Transplants in the Central Nervous
815 System. Stem Cells Transl Med. 2017 May;6(5).
816 23. Tomov N, Surchev L, Wiedenmann C, Döbrössy M, Nikkhah G.
817 Roscovitine, an experimental CDK5 inhibitor, causes delayed suppression
818 of microglial, but not astroglial recruitment around intracerebral
819 dopaminergic grafts. Exp Neurol. 2019 Aug;318.
820 24. Kikuchi T, Morizane A, Doi D, Magotani H, Onoe H, Hayashi T, et al.
821 Human iPS cell-derived dopaminergic neurons function in a primate
822 Parkinson's disease model. Nature. 2017 Aug 31;548(7669).
823 25. Clarke DJ, Branton RL. A Role for Tumor Necrosis Factor α in Death of
824 Dopaminergic Neurons Following Neural Transplantation. Exp Neurol.
825 2002 Jul;176(1).
826 26. Mirza B, Krook H, Andersson P, Larsson LC, Korsgren O, Widner H.
827 Intracerebral cytokine profiles in adult rats grafted with neural tissue of
828 different immunological disparity. Brain Res Bull. 2004 Mar;63(2).
829 27. Henn A, Lund S, Hedtjärn M, Schrattenholz A, Pörzgen P, Leist M. The
830 suitability of BV2 cells as alternative model system for primary microglia
831 cultures or for animal experiments examining brain inflammation. Vol. 26,
832 Altex. 2009.
833 28. Bossen C, Ingold K, Tardivel A, Bodmer J-L, Gaide O, Hertig S, et al.

Interactions of Tumor Necrosis Factor (TNF) and TNF Receptor Family Members in the Mouse and Human. J Biol Chem. 2006 May;281(20).

29. Bellucci A, Bubacco L, Longhena F, Parrella E, Faustini G, Porrini V, et al. Nuclear Factor-κB Dysregulation and α-Synuclein Pathology: Critical Interplay in the Pathogenesis of Parkinson's Disease. Front Aging Neurosci. 2020 Mar 24;12.

30. Seiz EG, Ramos-Gómez M, Courtois ET, Tønnesen J, Kokaia M, Liste Noya I, et al. Human midbrain precursors activate the expected developmental genetic program and differentiate long-term to functional A9 dopamine neurons in vitro. Enhancement by Bcl-XL. Exp Cell Res. 2012 Nov;318(19).

31. Lan X, Chen Q, Wang Y, Jia B, Sun L, Zheng J, et al. TNF-α Affects Human Cortical Neural Progenitor Cell Differentiation through the Autocrine Secretion of Leukemia Inhibitory Factor. PLoS One. 2012 Dec 7;7(12).

32. Herrmann M, Anders S, Straub RH, Jenei-Lanzl Z. TNF inhibits catecholamine production from induced sympathetic neuron-like cells in rheumatoid arthritis and osteoarthritis in vitro. Sci Rep. 2018 Dec 25;8(1).

33. Takahashi J. iPS cell-based therapy for Parkinson's disease: A Kyoto trial. Regen Ther. 2020 Mar;13.

34. Takahashi J. Clinical Trial for Parkinson's Disease Gets a Green Light in the US. Cell Stem Cell. 2021 Feb;28(2).

35. Brundin P, Karlsson J, Emgård M, Schierle GSK, Hansson O, Petersén Å, et al. Improving the Survival of Grafted Dopaminergic Neurons: A Review over Current Approaches. Cell Transplant. 2000 Mar 22;9(2).

859 36. Fischer R, Kontermann RE, Pfizenmaier K. Selective Targeting of TNF
860 Receptors as a Novel Therapeutic Approach. Front Cell Dev Biol. 2020
861 May 26;8.

862

863

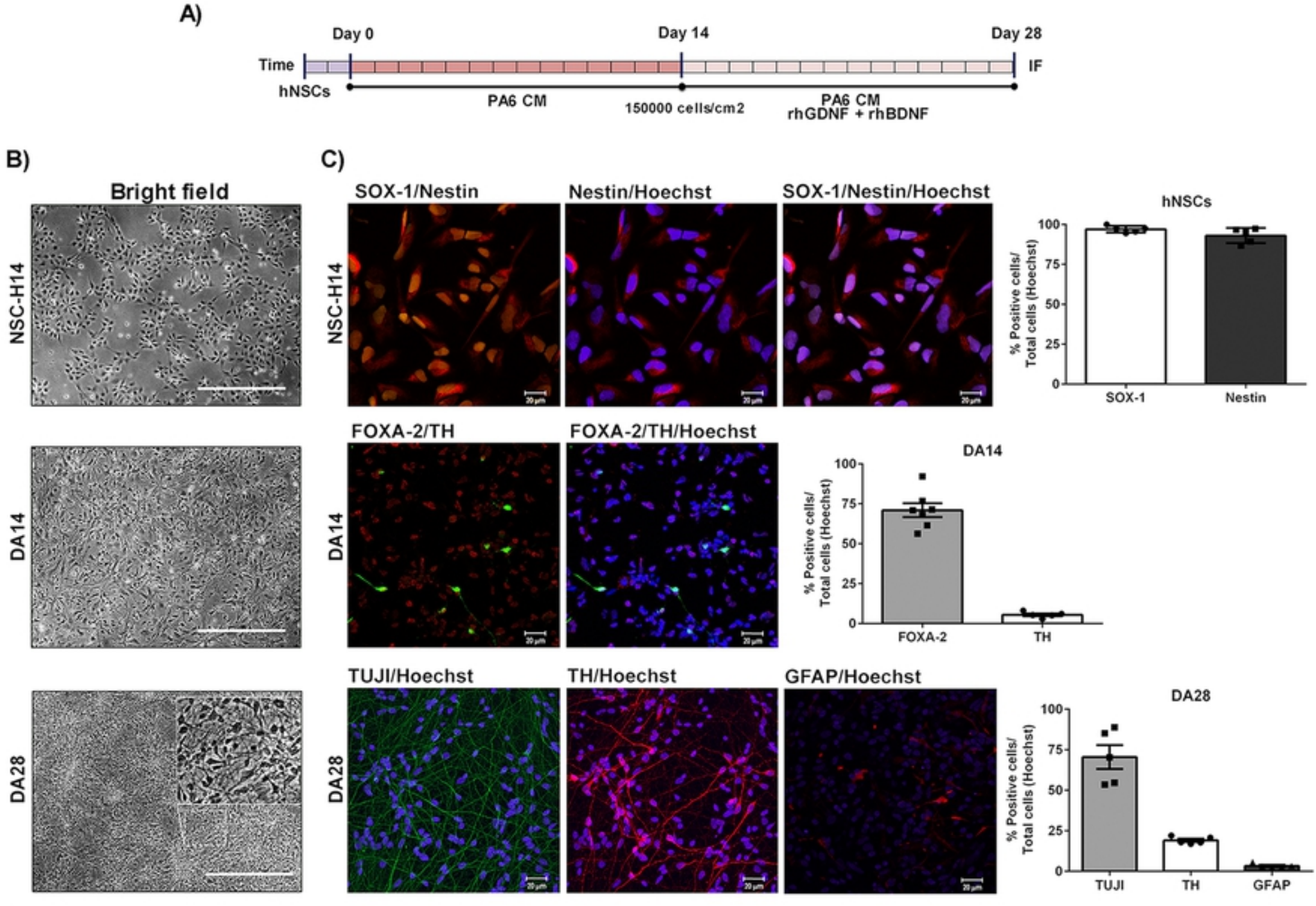
A)
Day 0
Day 14
Day 28
Time
IF
hNSCs
PA6 CM
150000 cells/cm2
PA6 CM
rhGDNF + rhBDNF
B)
Bright field
NSC-H14
DA14
DA28
C)
SOX-1/Nestin
Nestin/Hoechst
SOX-1/Nestin/Hoechst
NSC-H14
hNSCs
% Positive cells/
Total cells (Hoechst)
100
75
50
25
0
SOX-1
Nestin
FOXA-2/TH
FOXA-2/TH/Hoechst
DA14
DA14
% Positive cells/
Total cells (Hoechst)
FOXA-2
TH
TUJI/Hoechst
TH/Hoechst
GFAP/Hoechst
DA28
DA28
% Positive cells/
Total cells (Hoechst)
TUJI
TH
GFAP

Figure 1

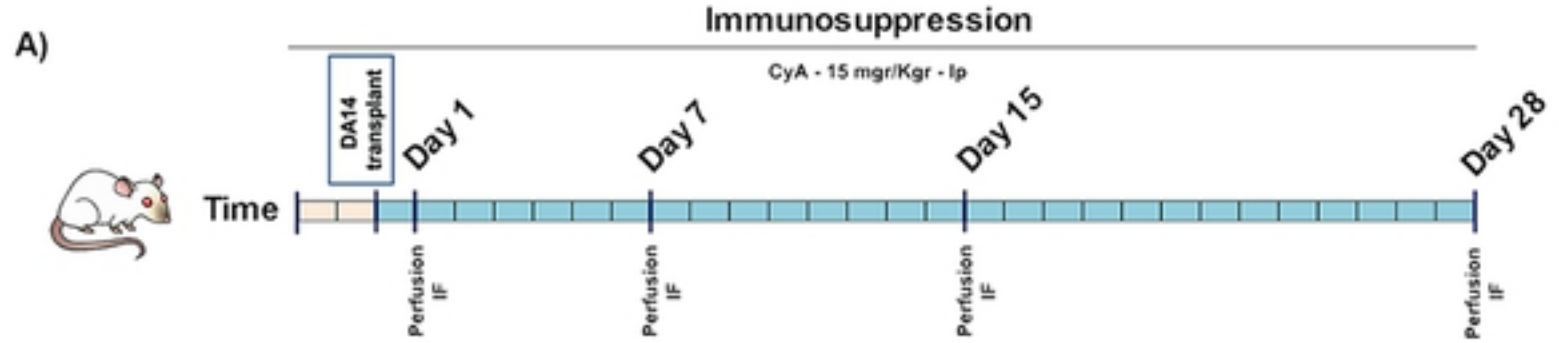

Cresyl violet staining
Immunofluorescence
Graft detection (hNCAM+ cells)
Cell counting for:
Neutrophils
Astrocytes (GFAP+ cells)
Microglial cells (MHC II+ cells)

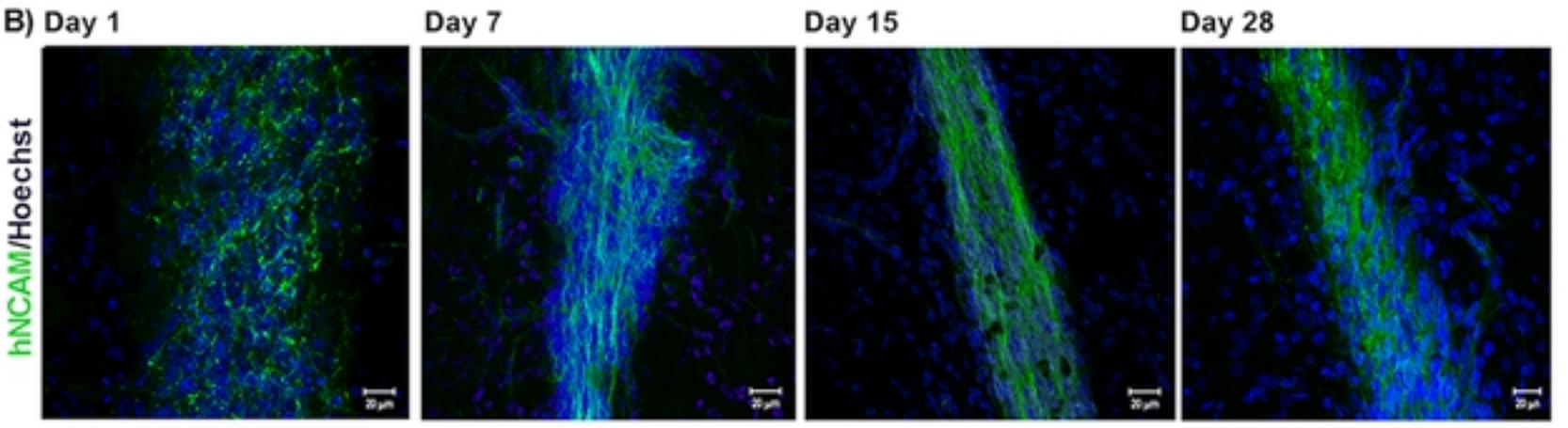

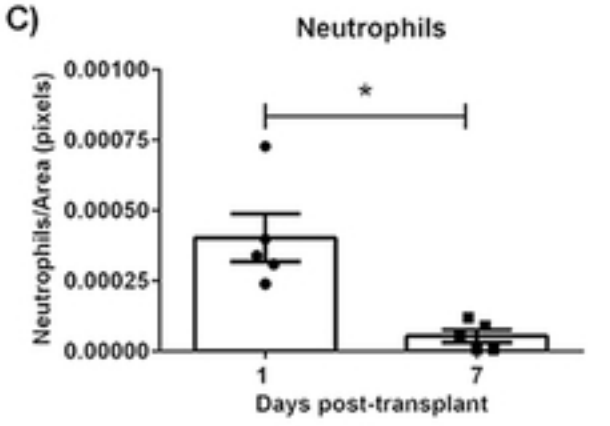

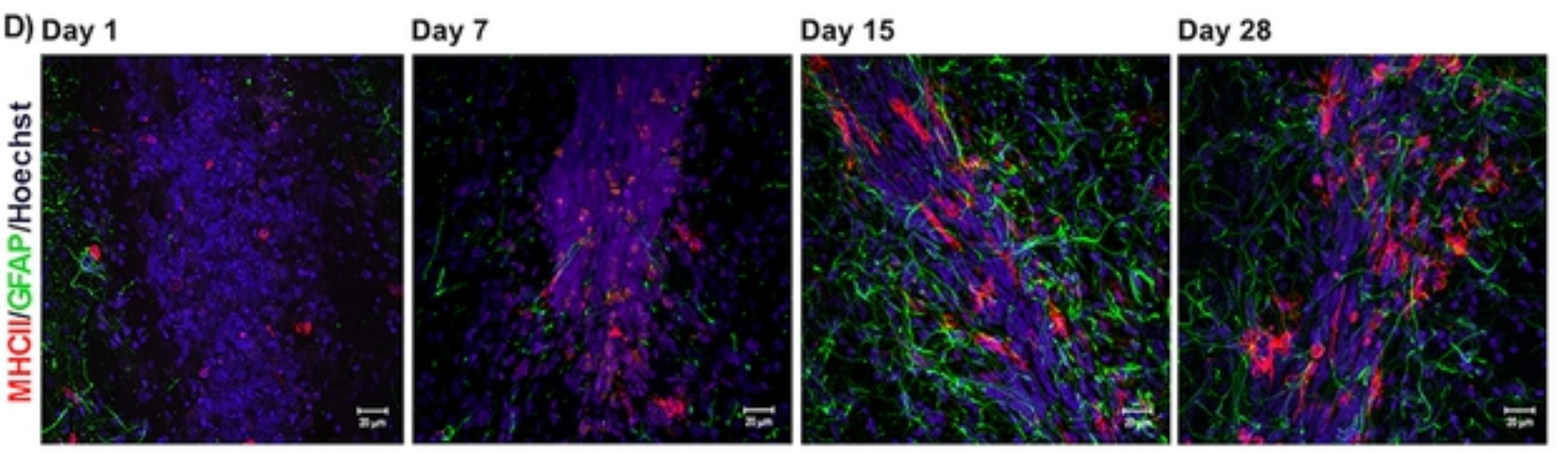

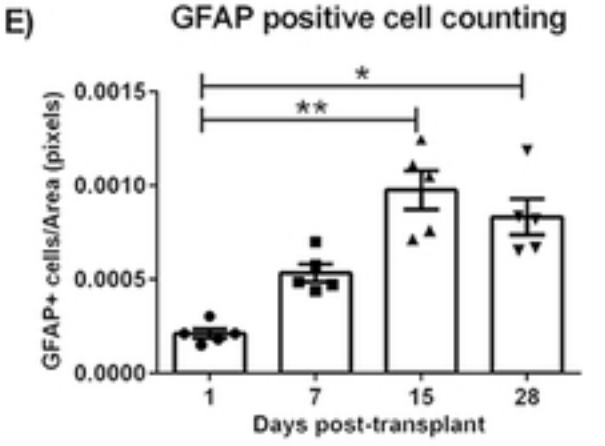

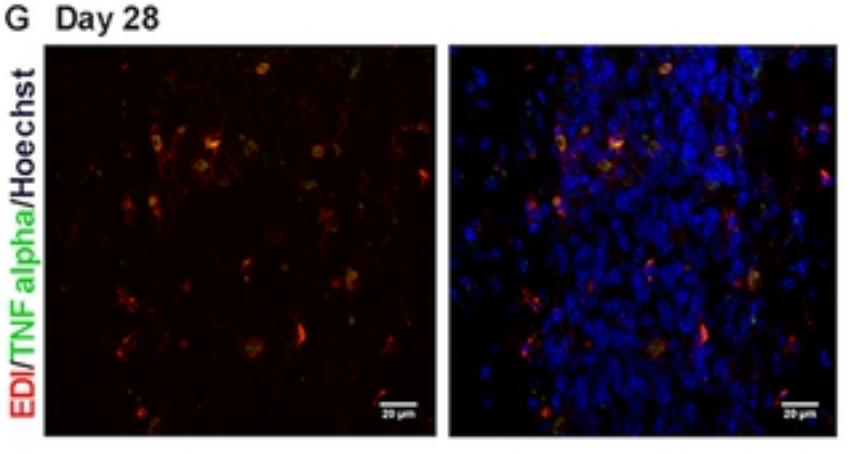

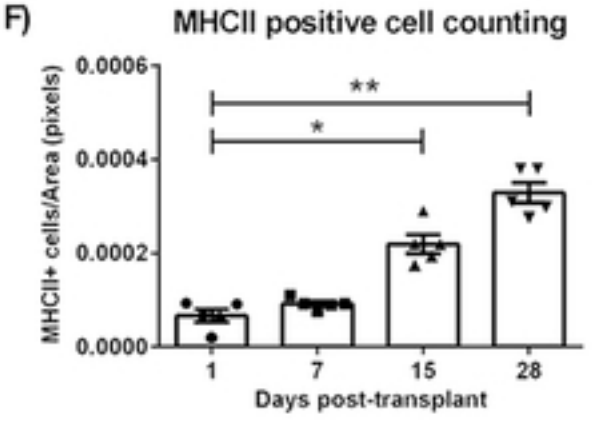

Figure 2

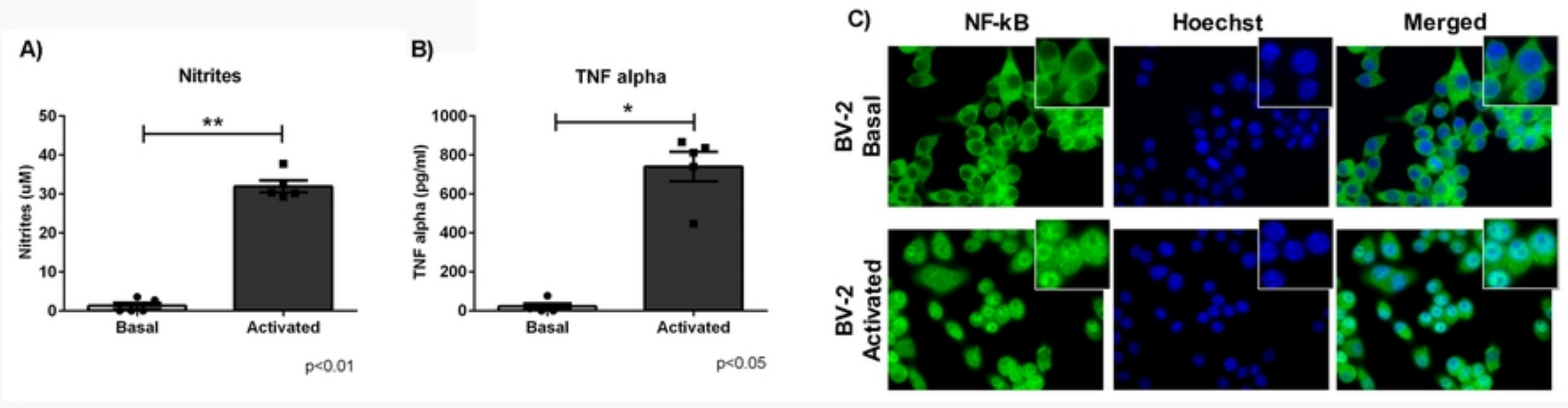
A)
Nitrites
Nitrites (uM)
50
40
30
20
10
0
**
Basal
Activated
p<0.01
B)
TNF alpha
TNF alpha (pg/ml)
1000
800
600
400
200
0
*
Basal
Activated
p<0.05
C)
NF-kB
Hoechst
Merged
BV-2 Basal
BV-2 Activated

Figure 3

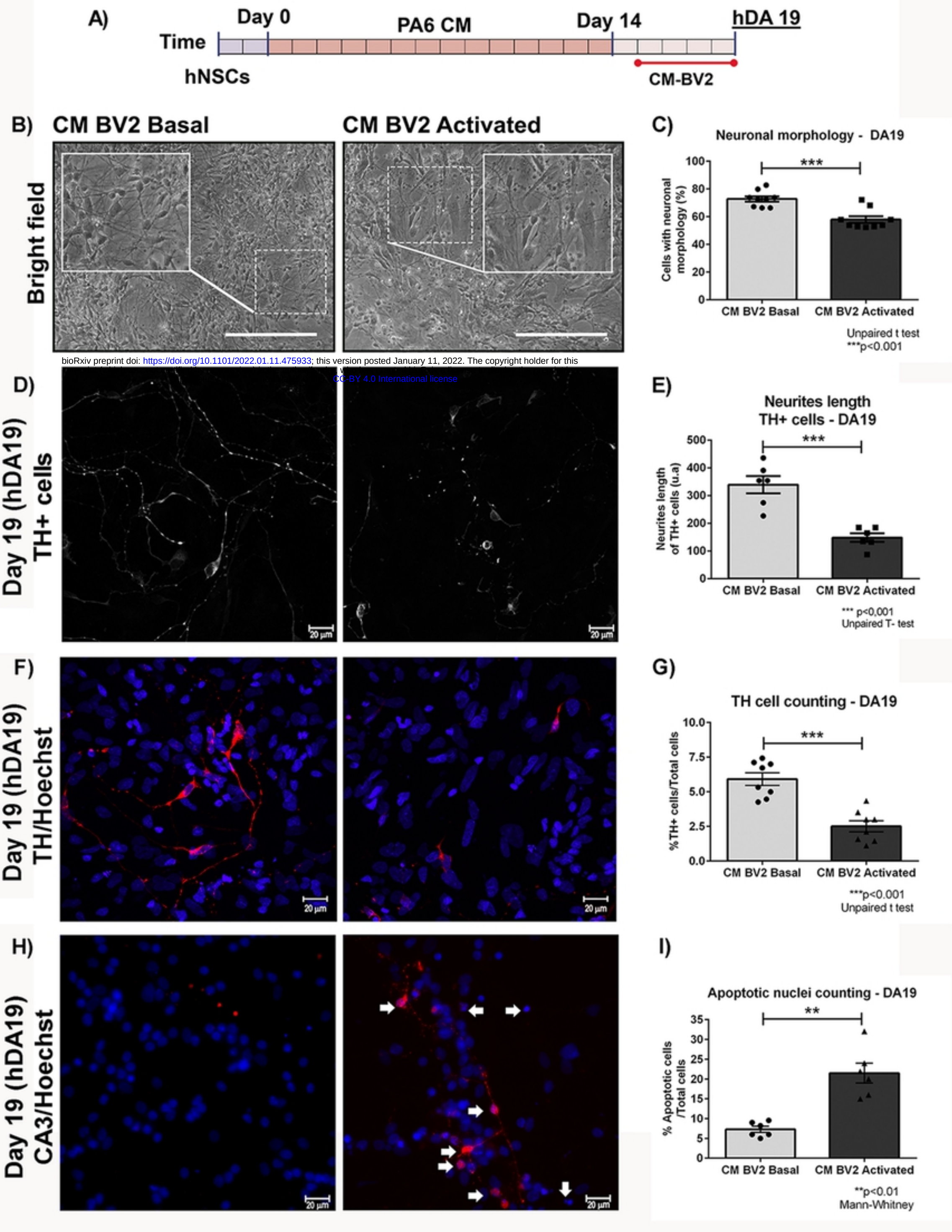

Figure 4

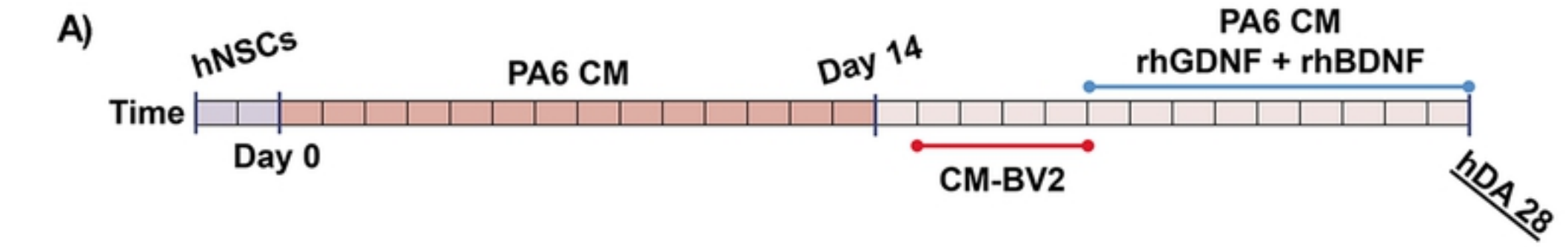

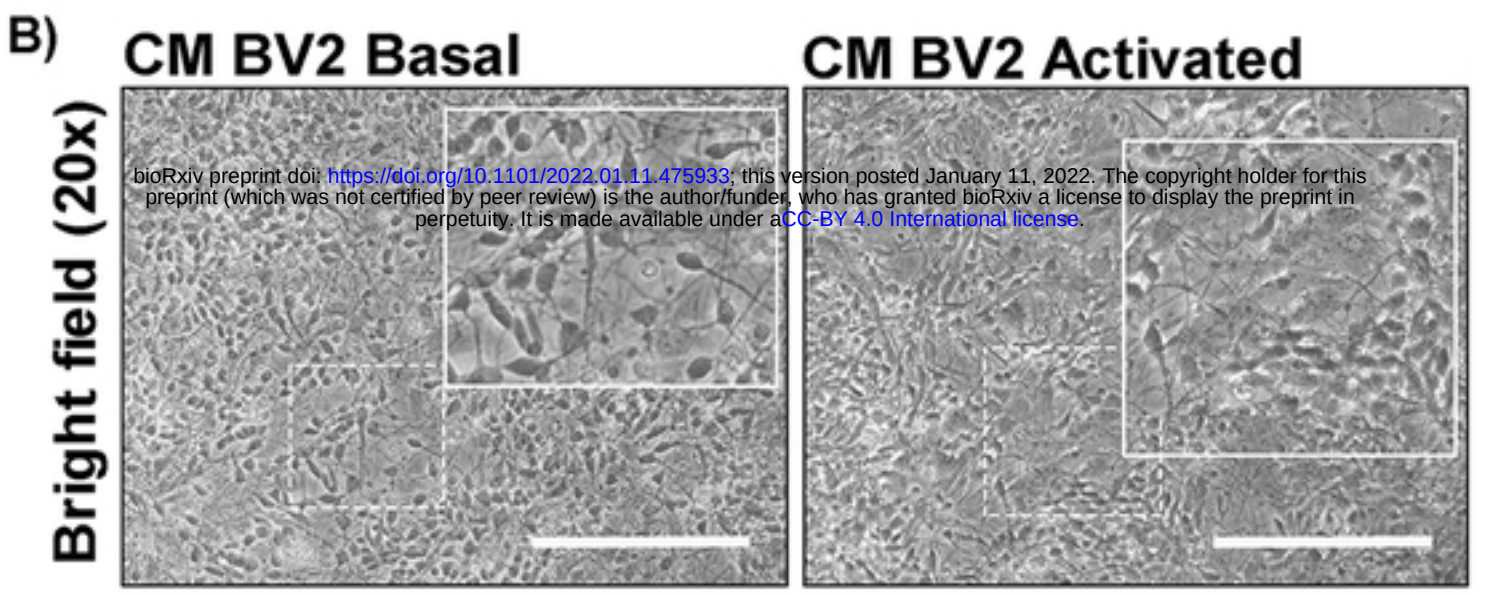

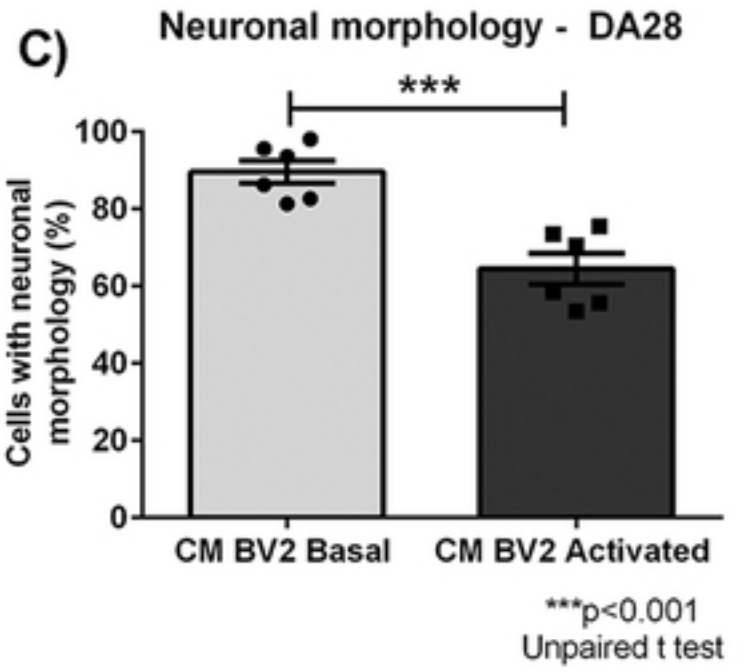

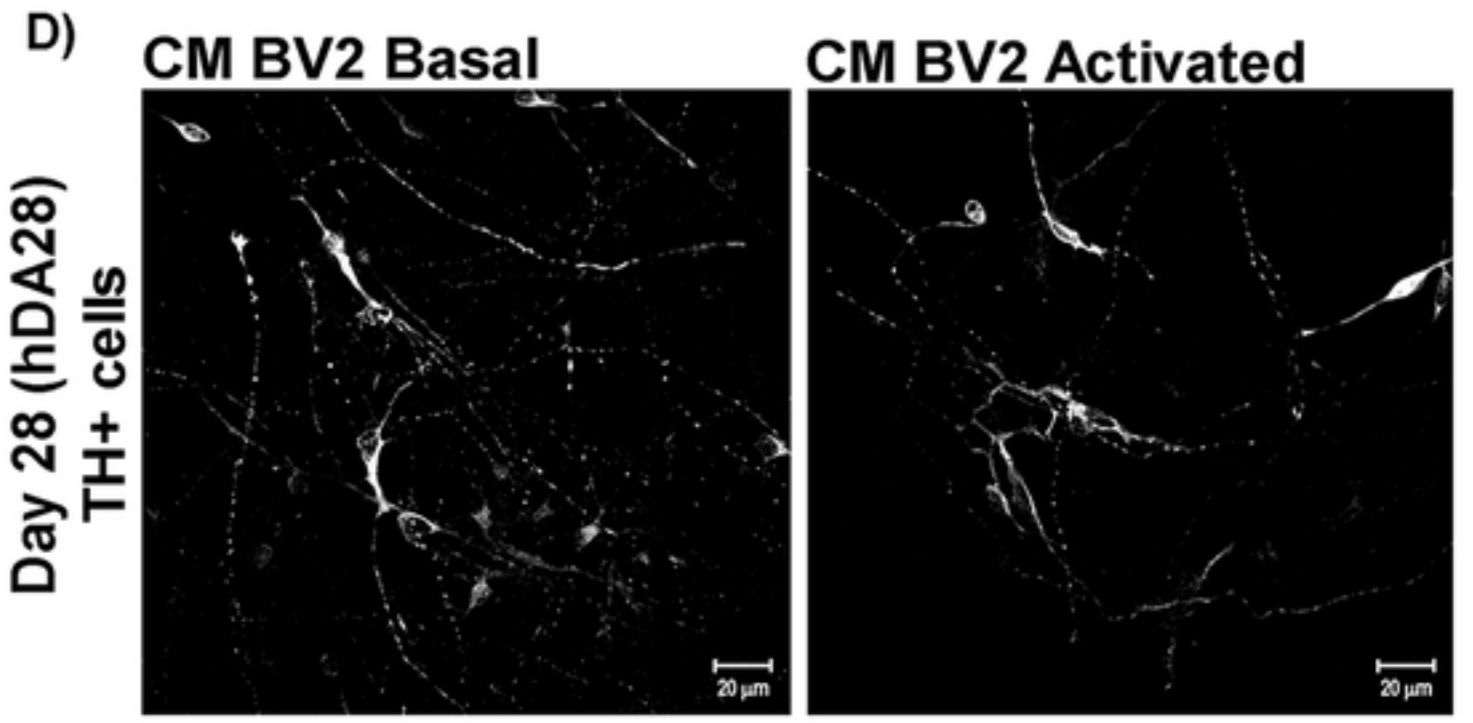

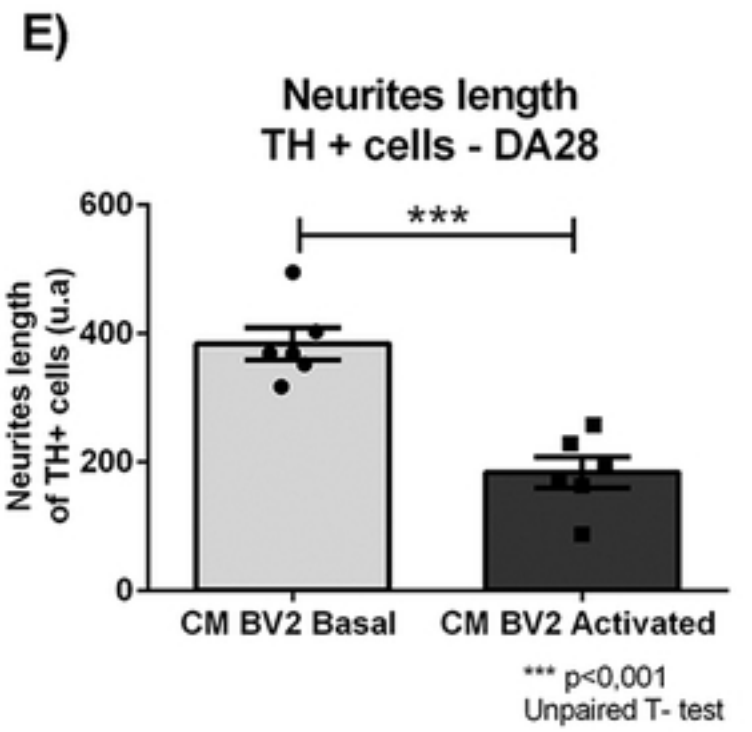

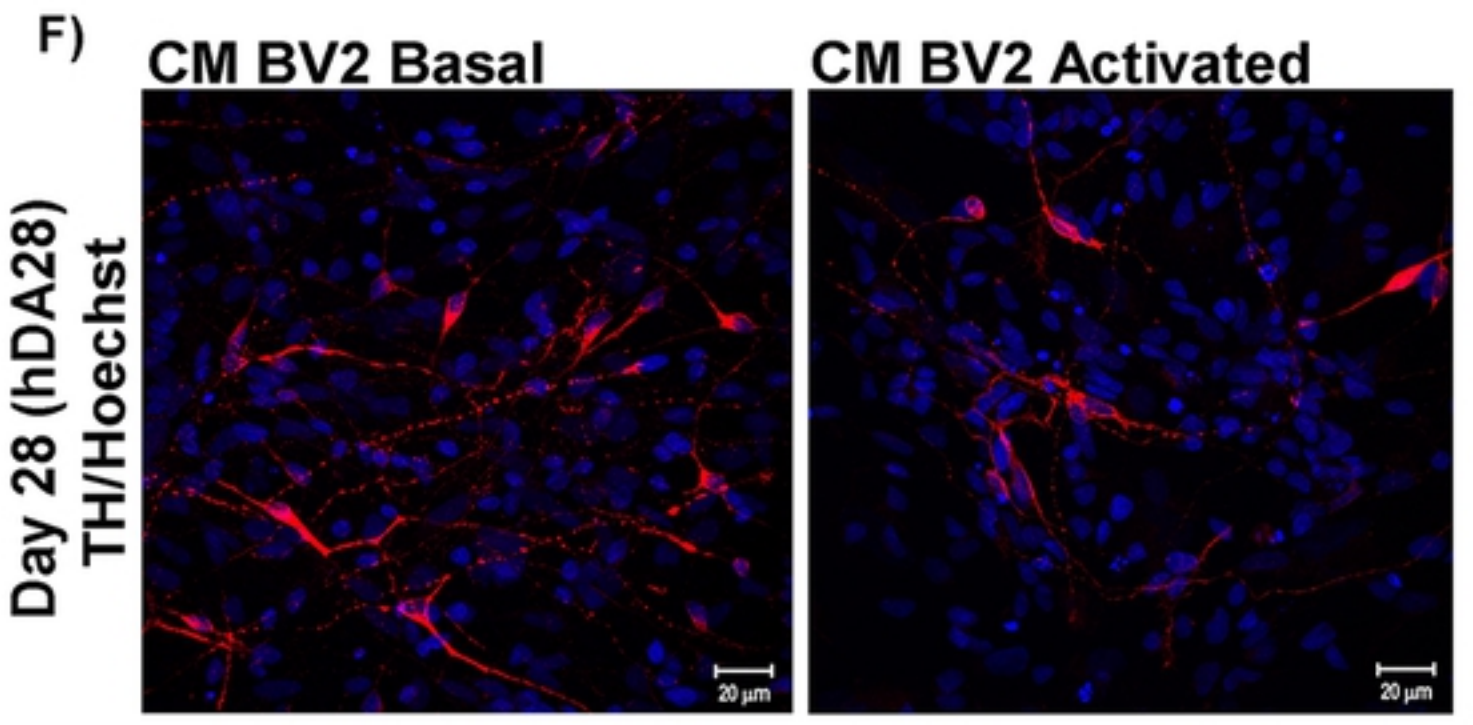

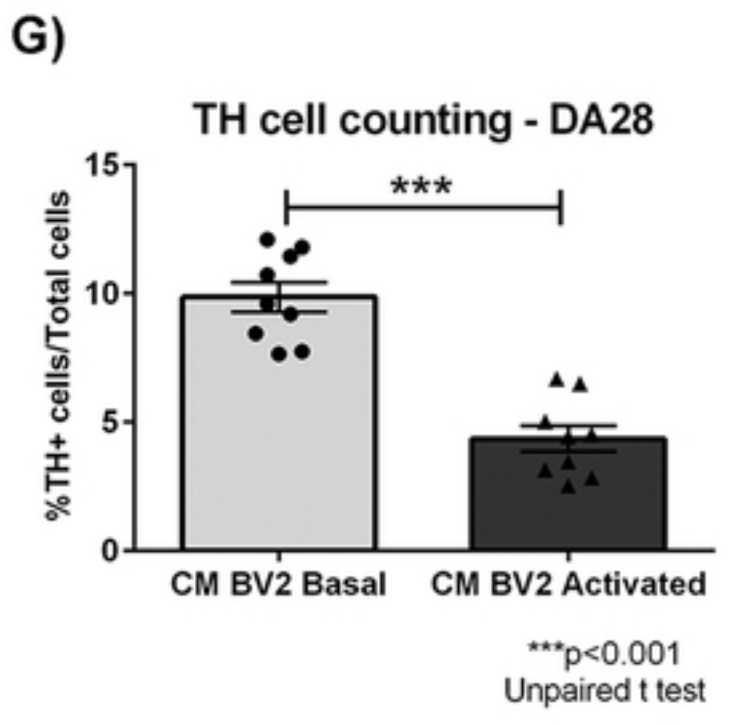

Figure 5

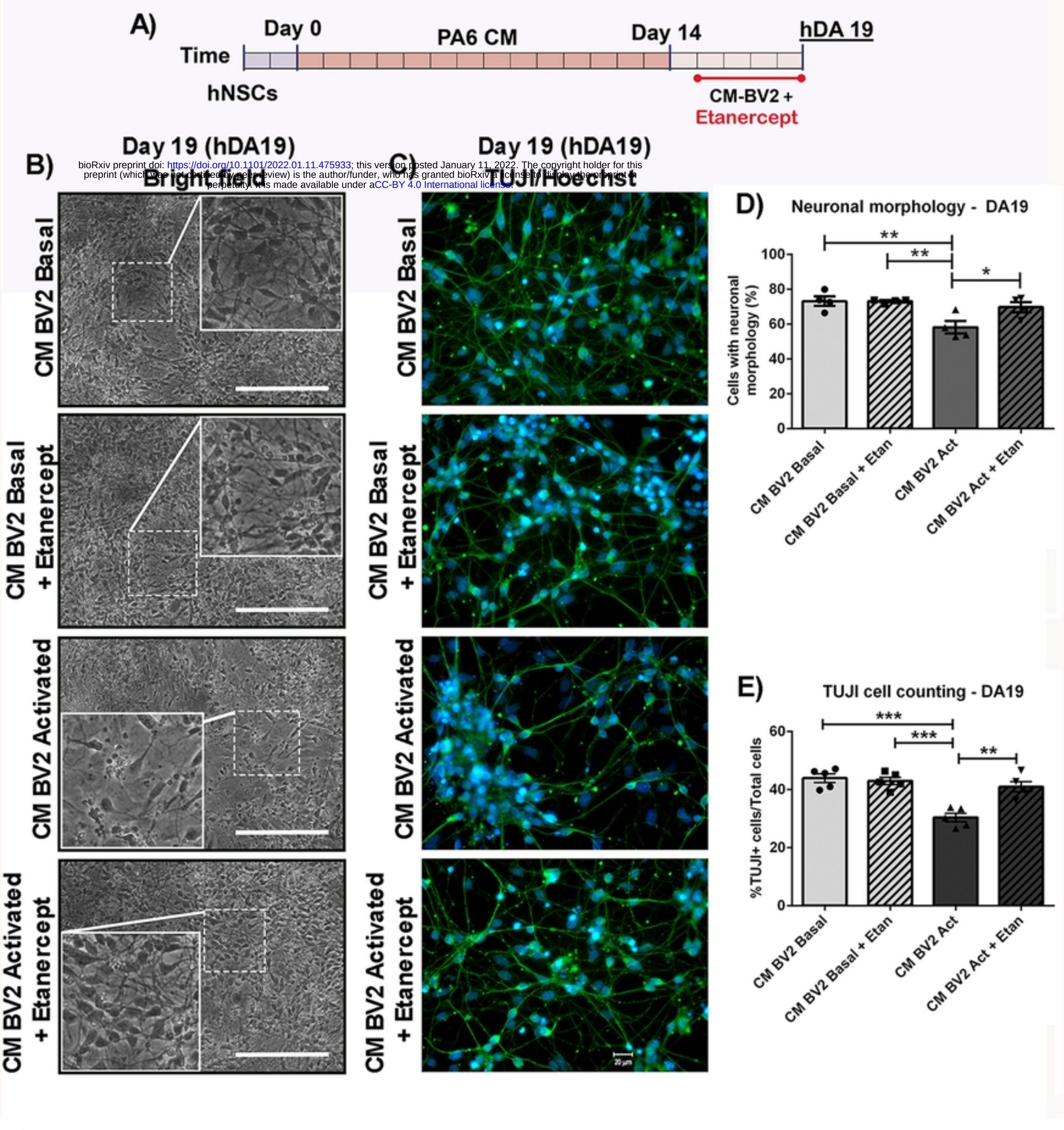

Figure 6

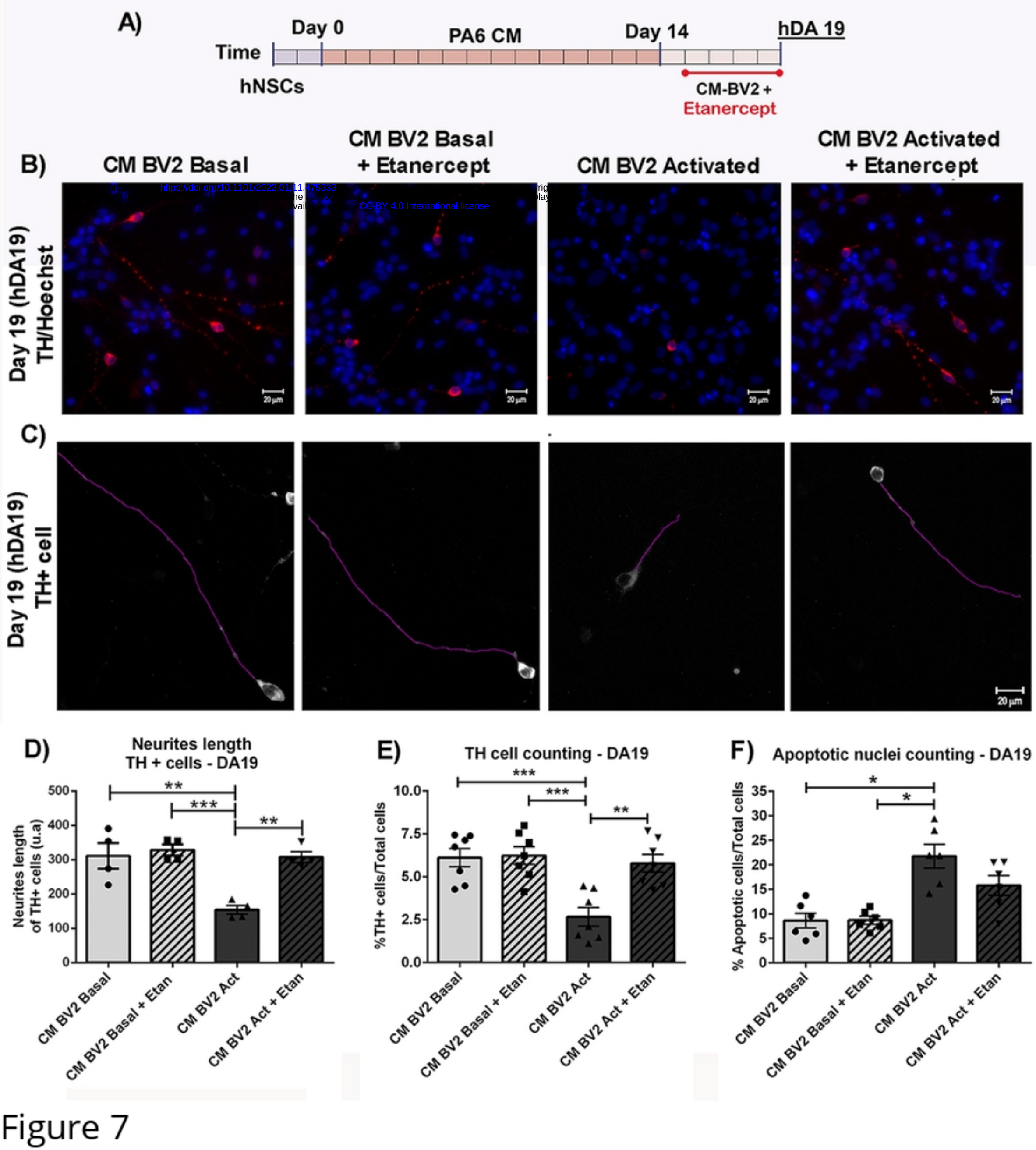

Figure 7

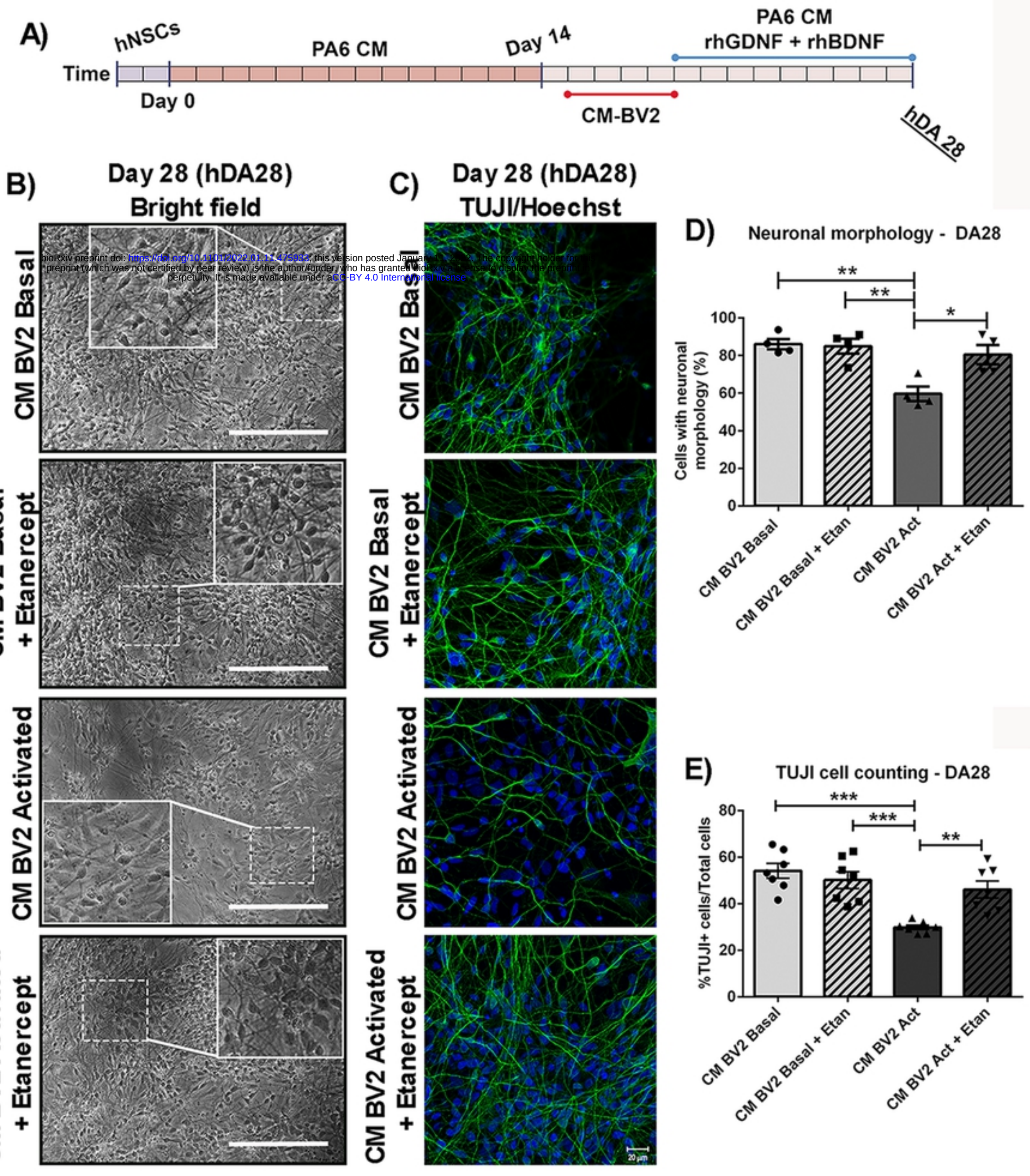

Figure 8

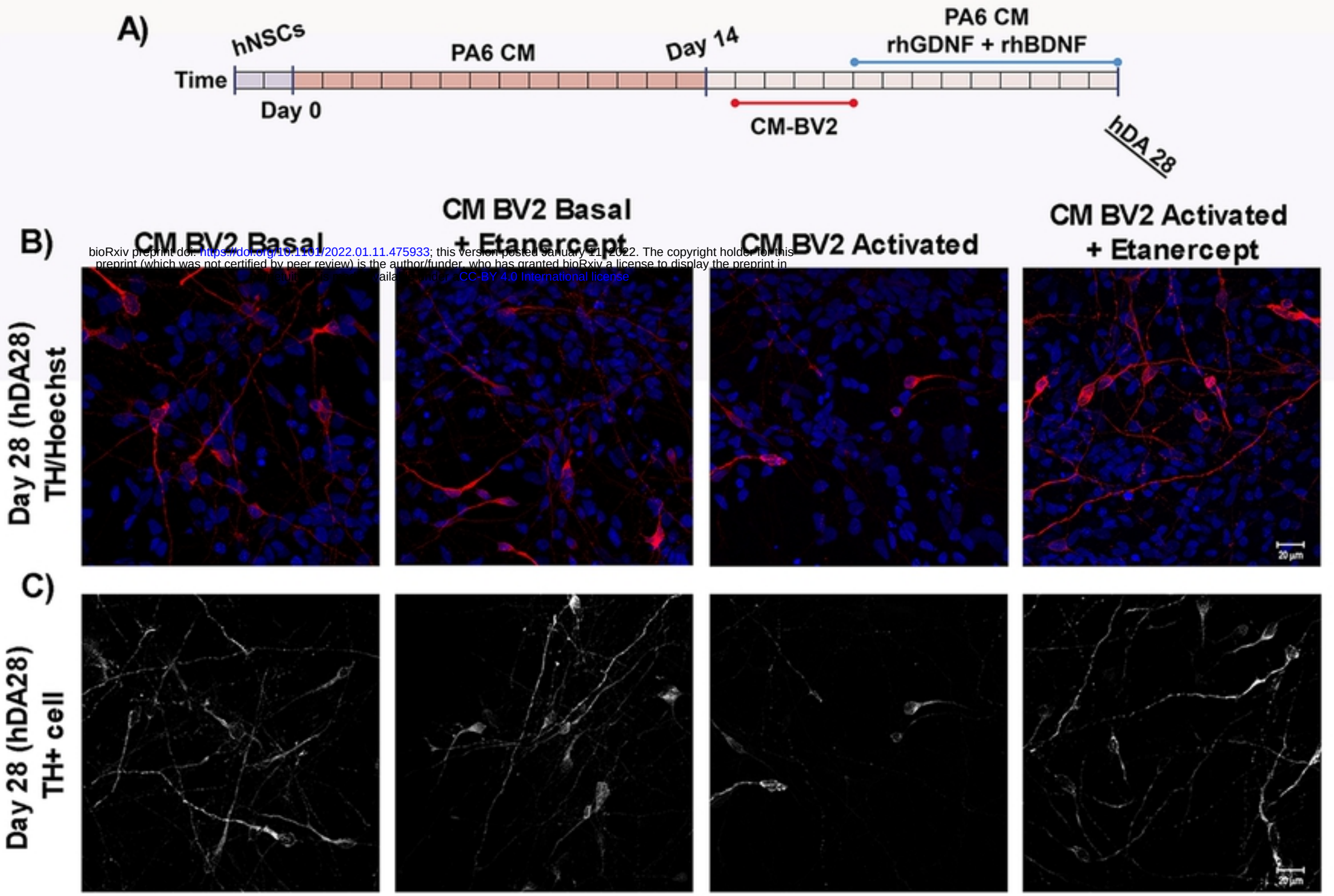

Figure 9